

# Observer-based Controller for VTOL-UAVs Tracking using Direct Vision-Aided Inertial Navigation Measurements

Hashim A. Hashim, Abdelrahman E.E. Eltoukhy, and Akos Odry

**Abstract**—This paper proposes a novel observer-based controller for Vertical Take-Off and Landing (VTOL) Unmanned Aerial Vehicle (UAV) designed to directly receive measurements from a Vision-Aided Inertial Navigation System (VA-INS) and produce the required thrust and rotational torque inputs. The VA-INS is composed of a vision unit (monocular or stereo camera) and a typical low-cost 6-axis Inertial Measurement Unit (IMU) equipped with an accelerometer and a gyroscope. A major benefit of this approach is its applicability for environments where the Global Positioning System (GPS) is inaccessible. The proposed VTOL-UAV observer utilizes IMU and feature measurements to accurately estimate attitude (orientation), gyroscope bias, position, and linear velocity. Ability to use VA-INS measurements directly makes the proposed observer design more computationally efficient as it obviates the need for attitude and position reconstruction. Once the motion components are estimated, the observer-based controller is used to control the VTOL-UAV attitude, angular velocity, position, and linear velocity guiding the vehicle along the desired trajectory in six degrees of freedom (6 DoF). The closed-loop estimation and the control errors of the observer-based controller are proven to be exponentially stable starting from almost any initial condition. To achieve global and unique VTOL-UAV representation in 6 DoF, the proposed approach is posed on the Lie Group and the design in unit-quaternion is presented. Although the proposed approach is described in a continuous form, the discrete version is provided and tested.

**Index Terms**—Vision-aided inertial navigation system, unmanned aerial vehicle, vertical take-off and landing, observer-based controller algorithm, landmark measurement, exponential stability.

## I. INTRODUCTION

IN the field of autonomous navigation, comprehensive autonomous modules able to accurately estimate Unmanned Aerial Vehicle (UAV) motion components and to provide control signals to successfully track the vehicle along the desired trajectory are in great demand. When using a Vision-Aided Inertial Navigation System (VA-INS) composed of a low-cost Inertial Measurement Unit (IMU) and a vision unit

(monocular or stereo camera), the UAV motion components that require estimation will include orientation (attitude), gyro bias, position, and linear velocity [1], [2]. Given the fact that rigid-body's attitude, position, and linear velocity are generally unknown, they can be reconstructed utilizing sensor measurements. UAV's orientation, commonly known as attitude, could be obtained through a set of inertial-frame observations in addition to the related body-frame measurements [3], [4]. However, it is crucial to note that widely available low-cost sensors produce uncertain measurements leading to poor attitude determination results. Therefore, alternative approaches, namely Gaussian filters [5]–[7] nonlinear filters [8]–[11], and neuro-adaptive filters [12], [13] have been proposed providing better estimates in comparison to [3], [4]. A common choice of sensor for attitude estimation is a low-cost 6-axis IMU composed of an accelerometer and a gyroscope. Moreover, an IMU integrated with a vision unit can supply pose (*i.e.*, attitude and position) information of a vehicle navigating with six degrees of freedom (6 DoF) [14]. Widely used methods of pose estimation include Gaussian filters [15], [16] and nonlinear filters [14], [17]. Nonetheless, pose estimation solutions in [14]–[17] produce good results only given the availability of linear velocity measurements obtained, for instance, by the Global Positioning System (GPS). In GPS-denied environments, however, rigid-body's linear velocity is challenging to obtain [2], [18]. Also, the solutions in [14]–[17] suppose that the accelerometer can supply the gravity measurements in the vehicle's body-frame assuming negligible linear accelerations. Several navigation solutions for acquiring rigid-body's attitude, position, and linear velocity in absence of GPS have been proposed that utilize IMU and feature measurements, namely indoor localization [19], [20], a Kalman filter [21], an extended Kalman filter [22], [23], an unscented Kalman filter [24], and a nonlinear navigation filter based on VA-INS [1], [2]. All of the above-listed solutions address solely the estimation stage, rather than proposing an estimator-based controller module.

Over the past few decades, UAVs, especially Vertical Take-Off and Landing (VTOL)-UAVs, have become widely used stimulating interest in and demand for UAV control solutions. Examples of such solutions include backstepping control [25], cascaded control [26], [27], sliding mode control [28], [29], hierarchical control [30], formation control [27], gain scheduling [31], and prescribed performance [32], among others. In spite of a significant effort made in [25], [26], [28]–[31] to control the rigid-body's pose, these solutions are heavily reliant on precise knowledge of rigid-body's attitude,

This work was supported in part by National Sciences and Engineering Research Council of Canada (NSERC), under the grants RGPIN-2022-04937, and in part by the Hong Kong Polytechnic University under grant P0036181 and RGC Hong Kong.

H. A. Hashim is with the Department of Mechanical and Aerospace Engineering, Carleton University, Ottawa, Ontario, K1S-5B6, Canada, email: hhashim@carleton.ca

A. E.E. Eltoukhy is with the Department of Industrial and Systems Engineering, The Hong Kong Polytechnic University, Hung Hum, Hong Kong, e-mail: abdelrahman.eltoukhy@polyu.edu.hk

A. Odry is with the Department of Mechatronics and Automation, Faculty of Engineering, University of Szeged, Moszkvai krt. 9, 6725 Szeged, Hungary

position, and angular velocity. As previously stated, attitude and position can be obtained using pose estimators known to produce good estimates, but yet these estimates are not sufficiently accurate to ensure a safe control process. In addition, angular velocity measurements supplied by a low-cost IMU module are uncertain and are likely to be corrupted with unknown bias [2], [18]. As such, applying the tracking control proposed in [25], [26], [28]–[31] to the information provided by a low-cost VA-INS module will in all likelihood produce undesirable results potentially causing a UAV to become unstable. Standalone observer and controller designs cannot guarantee the interconnected observer-based controller module stability [18].

Controlling the UAV trajectory in presence of uncertain and bias-corrupted measurements can be made possible by applying the image-based visual servoing (IBVS) approach combined with an IMU module able to collect the necessary UAV motion components, namely attitude, position, and angular velocity [2]. Examples of the above approach include an autonomous landing of a VTOL-UAV using IBVS and sliding mode control [33], output-feedback control for VTOL-UAV [34], [35], cascaded control for a quadrotor [36], model predictive control [37], and a linear observer coupled with a translation and attitude controller [38]. The common feature of the above-mentioned techniques [33]–[38] is a double loop structure reliant on Euler angles. The inner loop controls the angular velocity using IMU data, whereas the outer stage controls the thrust utilizing the vision measurements. The use of Euler angles helps to visualize the three-dimensional orientation of a rigid-body. However, the main weaknesses of the Euler angle representation are the singularity at several configurations and inability to represent the attitude globally [39], [40]. Although unit-quaternion is not subject to singularity, it suffers from non-uniqueness [39], [40]. *Lie Group*, in contrast, provides a nonsingular and unique representation of the rigid-body's orientation [8], [9]. Considering the nonlinearity of the VTOL-UAV model dynamics and the limitations of the Euler angles, the techniques in [33]–[38] are unable to guarantee global stability. A full-state observer-based controller on the *Lie Group* can be employed for VTOL-UAVs to resolve Euler angles singularities and non-uniqueness of unit-quaternion [18]. However, the approaches in [18], [33], [34], [36]–[38] require UAV pose reconstruction, which leads to a significant increase in the computational cost. Moreover, attitude and position reconstructions performed based on low-cost VA-INS measurements can be unreliable due to high levels of uncertainties [2], [14]. Considering the aforementioned limitations of the existing state-of-the-art solutions, it becomes apparent that UAV observer-based controllers able to use VA-INS measurements directly are in great demand. To this end, the contributions of this paper are as follows:

- A framework that allows for direct implementation of VA-INS measurements by a VTOL-UAV observer and controller has been established.
- A novel direct VA-INS-based nonlinear observer on the Lie Group that follows the true VTOL-UAV motion kinematics without the need for attitude and position

reconstructions has been developed;

- The proposed observer successfully estimates the VTOL-UAV's attitude, gyro-bias (IMU uncertain measurements), position, and linear velocity guaranteeing almost global exponential stability of the error signals starting from almost any initial condition; and
- Novel control laws based on and tightly-coupled with the proposed VA-INS-based nonlinear observer, are developed to control the UAV's attitude, position, angular velocity, and linear velocity guaranteeing almost global exponential stability of the closed-loop error signals starting from almost any initial condition.

To the best of the authors knowledge, observer-based controllers for VTOL-UAVs able to directly use VA-INS measurements without attitude and position reconstructions guaranteeing almost global exponential stability remain an unaddressed challenge.

This paper is composed of seven Sections. Section II gives an overview of *Lie Group*, math notation, identities, establishes the problem, and introduces the available VA-INS measurements. Section III presents a direct nonlinear observer for a VTOL-UAV in a continuous form. Section IV introduces a novel control strategy for VTOL-UAV in a continuous form. Section V presents the implementation details in a discrete form. Section VI depicts the effectiveness of the proposed methodology. Lastly, Section VII summarizes the work.

## II. PRELIMINARIES AND PROBLEM FORMULATION

### A. Preliminaries and Notation

In this paper, the set of real numbers is described by  $\mathbb{R}$ , an  $a$ -by- $b$  real dimensional space is represented by  $\mathbb{R}^{a \times b}$ , and non-negative real numbers are denoted by  $\mathbb{R}_+$ .  $\|y\| = \sqrt{y^\top y}$  refers to Euclidean norm of a vector  $y \in \mathbb{R}^a$ .  $\mathbf{I}_a$  refers to an  $a$ -by- $a$  identity matrix, and  $0_{a \times b}$  denotes an  $a$ -by- $b$  zero matrix.  $\lambda(W) = \{\lambda_1, \lambda_2, \dots, \lambda_a\}$  stands for the set of eigenvalues of  $W \in \mathbb{R}^{a \times a}$  with  $\bar{\lambda}_W = \bar{\lambda}(W)$  being the set's maximum value and  $\underline{\lambda}_W = \underline{\lambda}(W)$  being the set's minimum value. Consider a UAV-VTOL traveling in 6 DoF where

- $\{\mathcal{B}\} = \{e_{B1}, e_{B2}, e_{B3}\}$  denotes the vehicle's body-frame and
- $\{\mathcal{I}\} = \{e_1, e_2, e_3\}$  refers to a fixed inertial-frame such that  $e_1 := [1, 0, 0]^\top$ ,  $e_2 := [0, 1, 0]^\top$ , and  $e_3 := [0, 0, 1]^\top$ .

$\mathbb{SO}(3)$  denotes *Special Orthogonal Group* defined by

$$\mathbb{SO}(3) = \{R \in \mathbb{R}^{3 \times 3} \mid RR^\top = R^\top R = \mathbf{I}_3, \det(R) = +1\}$$

where  $R \in \mathbb{SO}(3)$  is vehicle's orientation, also known as attitude.  $\mathfrak{so}(3)$  describes the *Lie-algebra* of  $\mathbb{SO}(3)$  such that

$$\mathfrak{so}(3) = \{[\Omega]_\times \in \mathbb{R}^{3 \times 3} \mid [\Omega]_\times^\top = -[\Omega]_\times\}$$

where

$$[\Omega]_\times = \begin{bmatrix} 0 & -\Omega_3 & \Omega_2 \\ \Omega_3 & 0 & -\Omega_1 \\ -\Omega_2 & \Omega_1 & 0 \end{bmatrix} \in \mathfrak{so}(3), \quad \Omega = \begin{bmatrix} \Omega_1 \\ \Omega_2 \\ \Omega_3 \end{bmatrix}$$

$\text{vex} : \mathfrak{so}(3) \rightarrow \mathbb{R}^3$  defines the map of  $[\cdot]_\times$  to  $\mathbb{R}^3$  where  $\text{vex}([\Omega]_\times) = \Omega$  for all  $\Omega \in \mathbb{R}^3$ .  $\mathcal{P}_a : \mathbb{R}^{3 \times 3} \rightarrow \mathfrak{so}(3)$

is the anti-symmetric projection operator, while  $\Upsilon(\cdot)$  is a composition mapping of  $\text{vex} \circ \mathcal{P}_a$  given by

$$\mathcal{P}_a(M) = \frac{1}{2}(M - M^\top) \in \mathfrak{so}(3), \quad \forall M \in \mathbb{R}^{3 \times 3} \quad (1)$$

$$\Upsilon(M) = \text{vex}(\mathcal{P}_a(M)) \in \mathbb{R}^3, \quad \forall M \in \mathbb{R}^{3 \times 3} \quad (2)$$

Define the following map:

$$\|R\|_I = \frac{1}{4} \text{Tr}\{\mathbf{I}_3 - R\} \in [0, 1], \quad R \in \mathbb{SO}(3) \quad (3)$$

Define  $\mathbb{SE}_2(3) = \mathbb{SO}(3) \times \mathbb{R}^3 \times \mathbb{R}^3 \subset \mathbb{R}^{5 \times 5}$  [41] as the extended *Special Euclidean Group* where

$$\mathbb{SE}_2(3) = \{X \in \mathbb{R}^{5 \times 5} \mid R \in \mathbb{SO}(3), P, V \in \mathbb{R}^3\} \quad (4)$$

$$X = f(R^\top, P, V) = \begin{bmatrix} R^\top & P & V \\ 0_{1 \times 3} & 1 & 0 \\ 0_{1 \times 3} & 0 & 1 \end{bmatrix} \in \mathbb{SE}_2(3) \quad (5)$$

such that  $X$  is the homogeneous navigation matrix and  $R$ ,  $P$ , and  $V$  describe the vehicle's attitude, position, and linear velocity, respectively [1], [2], [18], [41]. One has

$$X^{-1} = \begin{bmatrix} R & -RP & -RV \\ 0_{1 \times 3} & 1 & 0 \\ 0_{1 \times 3} & 0 & 1 \end{bmatrix} \in \mathbb{SE}_2(3)$$

Let  $\mathcal{U}_M = \mathfrak{so}(3) \times \mathbb{R}^3 \times \mathbb{R}^3 \times \mathbb{R} \subset \mathbb{R}^{5 \times 5}$  be defined as

$$\mathcal{U}_M = \{u([\Omega]_\times, V, e_3, \kappa) \mid [\Omega]_\times \in \mathfrak{so}(3), V, e_3 \in \mathbb{R}^3, \kappa \in \mathbb{R}\} \quad (6)$$

$$U = u([\Omega]_\times, V, e_3, \kappa) = \begin{bmatrix} [\Omega]_\times & V & e_3 \\ 0_{1 \times 3} & 0 & 0 \\ 0_{1 \times 3} & \kappa & 0 \end{bmatrix} \in \mathcal{U}_M$$

To learn more about the group  $\mathbb{SE}_2(3)$ , the navigation matrix  $X \in \mathbb{SE}_2(3)$ , and  $\mathcal{U}_M$  consult [1], [2], [18]. The following identity is used throughout this paper:

$$\text{Tr}\{N[\Omega]_\times\} = \text{Tr}\{\mathcal{P}_a(N)[\Omega]_\times\}, \quad \Omega \in \mathbb{R}^3, N \in \mathbb{R}^{3 \times 3} \quad (7)$$

$$= -2\text{vex}(\mathcal{P}_a(N))^\top \Omega$$

$$[y \times z]_\times = zy^\top - yz^\top, \quad y, z \in \mathbb{R}^3 \quad (8)$$

## B. Problem Formulation

Let  $R \in \mathbb{SO}(3)$ ,  $P \in \mathbb{R}^3$ , and  $V \in \mathbb{R}^3$  be the true attitude, position, and linear velocity of a VTOL-UAV traveling in 6 DoF, respectively.  $R$ ,  $P$ , and  $V$  are assumed to be completely unknown. The VTOL-UAV motion equations are as follows [18]:

$$\begin{cases} \dot{R} &= -[\Omega]_\times R \\ J\dot{\Omega} &= [J\Omega]_\times \Omega + \mathcal{T} \end{cases}, \quad R, \Omega, \mathcal{T} \in \{\mathcal{B}\} \quad (9)$$

$$\begin{cases} \dot{P} &= V \\ \dot{V} &= ge_3 - \frac{\mathfrak{S}}{m} R^\top e_3 \end{cases}, \quad P, V \in \{\mathcal{I}\} \quad (10)$$

where  $\Omega \in \mathbb{R}^3$ ,  $J \in \mathbb{R}^{3 \times 3}$ ,  $m \in \mathbb{R}$ ,  $g \in \mathbb{R}$ , and  $e_3 = [0, 0, 1]^\top$  describe angular velocity, a constant symmetric positive definite inertia matrix, UAV's mass, gravitational acceleration, and a basis vector, respectively. Also,  $\mathcal{T} \in \mathbb{R}^3$  and  $\mathfrak{S} \in \mathbb{R}$  refer to rotational torque input and thrust input, respectively. In view

of (9) and (10), the VTOL-UAV motion nonlinear equations can be re-expressed as

$$\begin{cases} \dot{X} &= XU - \mathcal{G}X \\ J\dot{\Omega} &= [J\Omega]_\times \Omega + \mathcal{T} \end{cases}, \quad U, \mathcal{G} \in \mathcal{U}_M, X \in \mathbb{SE}_2(3) \quad (11)$$

where, based on the definition in (5) and (6),  $X$  is the navigation matrix,

$$U = u([\Omega]_\times, 0_{3 \times 3}, -\frac{\mathfrak{S}}{m} e_3, 1) = \begin{bmatrix} [\Omega]_\times & 0_{3 \times 3} & -\frac{\mathfrak{S}}{m} e_3 \\ 0_{1 \times 3} & 0 & 0 \\ 0_{1 \times 3} & 1 & 0 \end{bmatrix}$$

and  $\mathcal{G} = u(0_{3 \times 3}, 0_{3 \times 3}, -ge_3, 1)$ . Therefore, it can be shown that the dynamics in (11) have the map  $\mathbb{SE}_2(3) \times \mathcal{U}_M \rightarrow T_X \mathbb{SE}_2(3) \in \mathbb{R}^{5 \times 5}$  where  $\dot{X} \in T_X \mathbb{SE}_2(3)$ . Attitude and position of a UAV can be extracted through a group of observations in  $\{\mathcal{I}\}$  and the corresponding measurements in  $\{\mathcal{B}\}$  [14]. Let  $p_i$  denote the  $i$ th known inertial-frame feature observation. The respective  $i$ th body-frame feature measurement is given by [1], [14]

$$y_i = R(p_i - P) + b_i \in \mathbb{R}^3, \quad \forall i = 1, \dots, n \quad (12)$$

where  $b_i$  describes an unknown uncertainty.

**Assumption 1.** (*UAV attitude and position observability*) The attitude  $R \in \mathbb{SO}(3)$  and position  $P \in \mathbb{R}^3$  of a UAV can be defined if there are three or more non-collinear observations and their measurements defined in (12).

Assumption 1 is common for problems involving attitude and position estimation [14], [17].

**Lemma 1.** [8] Let  $R \in \mathbb{SO}(3)$ ,  $M = M^\top \in \mathbb{R}^{3 \times 3}$  where  $\text{rank}(M) \geq 2$ , and  $\bar{M} = \text{Tr}\{M\}\mathbf{I}_3 - M$ . Thereby, the following two definitions hold:

$$\|\Upsilon(R)\|^2 = 4(1 - \|R\|_I)\|R\|_I \quad (13)$$

$$\frac{\lambda_M^2}{\lambda_{\bar{M}}^2} \|R\|_I \leq \|\Upsilon(RM)\|^2 \leq \frac{\lambda_M^2}{\lambda_{\bar{M}}^2} \|R\|_I \quad (14)$$

**Definition 1.** [8] A forward invariant non-attractive set  $\mathcal{S}_u \subseteq \mathbb{SO}(3)$  is defined by

$$\mathcal{S}_u = \{R(0) \in \mathbb{SO}(3) \mid \text{Tr}\{R(0)\} = -1\} \quad (15)$$

with  $R(0) \in \mathcal{S}_u$  if one of the following three conditions holds:  $R(0) = \text{diag}(1, -1, -1)$ ,  $R(0) = \text{diag}(-1, 1, -1)$ , or  $R(0) = \text{diag}(-1, -1, 1)$ .

**Lemma 2.** (*Barbalat Lemma Extension*) Let  $x(t)$  be a solution of a differential equation  $\dot{x}(t) = f(t) + g(t)$  where  $f(t)$  is a uniformly continuous function. Suppose that  $\lim_{t \rightarrow \infty} x(t) = k_c$  and  $\lim_{t \rightarrow \infty} g(t) = 0$ , where  $k_c$  denotes a constant. Then,  $\lim_{t \rightarrow \infty} \dot{x}(t) = 0$ .

## III. DIRECT OBSERVER DESIGN ON LIE GROUP

This Section aims to design a nonlinear observer for a VTOL-UAV on the *Lie Group* that can be implemented using a group of measurements directly alleviating the necessity for attitude and position reconstruction. Define an angular velocity measurement obtained by a gyroscope as

$$\Omega_m = \Omega + b_\Omega \in \mathbb{R}^3 \quad (16)$$

where  $b_\Omega$  denotes unknown uncertainty (bias) of the gyro measurement (for more information about IMU visit [8]–[11]). Let  $b_\Omega$  be a positive constant, and let

$$\hat{X} = f(\hat{R}^\top, \hat{P}, \hat{V}) = \begin{bmatrix} \hat{R}^\top & \hat{P} & \hat{V} \\ 0_{1 \times 3} & 1 & 0 \\ 0_{1 \times 3} & 0 & 1 \end{bmatrix} \in \mathbb{SE}_2 \quad (3)$$

where  $\hat{R} \in \mathbb{SO}(3)$ ,  $\hat{b}_\Omega \in \mathbb{R}^3$ ,  $\hat{P} \in \mathbb{R}^3$ , and  $\hat{V} \in \mathbb{R}^3$  describe estimates of navigation matrix, attitude, gyro bias, position, and linear velocity, respectively. Define the error between the true and the estimated values as follows:

$$\tilde{R}_o = \hat{R}^\top R \quad (17)$$

$$\tilde{b}_\Omega = b_\Omega - \hat{b}_\Omega \quad (18)$$

$$\tilde{P}_o = \hat{P} - \tilde{R}_o P \quad (19)$$

$$\tilde{V}_o = \hat{V} - \tilde{R}_o V \quad (20)$$

where  $\tilde{R}_o$  is an attitude error,  $\tilde{b}_\Omega$  is a gyroscope error,  $\tilde{P}_o$  is a position error, and  $\tilde{V}_o$  is a linear velocity error for all  $\tilde{R}_o \in \mathbb{SO}(3)$  and  $\tilde{b}_\Omega, \tilde{P}_o, \tilde{V}_o \in \mathbb{R}^3$ . According to (17), (19), and (20), one finds that  $\tilde{X}_o = \hat{X} X^{-1} = f(\tilde{R}_o, \tilde{P}_o, \tilde{V}_o) \in \mathbb{SE}_2(3)$ .

#### A. Measurement Set-up

Let  $s_i$  denote the confidence level of the  $i$ th sensor measurement, and define  $s_T = \sum_{i=1}^n s_i$  such that Assumption 1 is met ( $n \geq 3$ ). Let  $y_i = R(p_i - P)$  and  $p_c = \frac{1}{s_T} \sum_{i=1}^n s_i p_i$ , and define  $M = \sum_{i=1}^n s_i (p_i - p_c)(p_i - p_c)^\top$  which can be easily transformed into  $M = \sum_{i=1}^n s_i p_i p_i^\top - s_T p_c p_c^\top$ . Therefore,

$$\begin{aligned} \sum_{i=1}^n s_i \hat{R}^\top y_i (p_i - p_c)^\top &= \sum_{i=1}^n s_i \hat{R}^\top R (p_i - P) (p_i - p_c)^\top \\ &= \tilde{R}_o \sum_{i=1}^n s_i (p_i p_i^\top - P p_i^\top - p_i p_c^\top + P p_c^\top) \\ &= \tilde{R}_o \left( \sum_{i=1}^n s_i p_i p_i^\top - s_T p_c p_c^\top \right) = \tilde{R}_o M \end{aligned} \quad (21)$$

Therefore, one shows

$$\begin{aligned} \mathcal{P}_a(\tilde{R}_o M) &= \mathcal{P}_a \left( \sum_{i=1}^n s_i \hat{R}^\top y_i (p_i - p_c)^\top \right) \\ &= \sum_{i=1}^n \frac{s_i}{2} \left( \hat{R}^\top y_i (p_i - p_c)^\top - (p_i - p_c) y_i^\top \hat{R} \right) \end{aligned} \quad (22)$$

Based on (2),  $\Upsilon(\tilde{R}_o M) = \text{vex}(\mathcal{P}_a(\tilde{R}_o M))$ . Consequently, one has

$$\Upsilon(\tilde{R}_o M) = \sum_{i=1}^n \frac{s_i}{2} \left( (p_i - p_c) \times \hat{R}^\top y_i \right) \quad (23)$$

Also, one finds

$$\begin{aligned} \sum_{i=1}^n s_i \tilde{y}_i &= \sum_{i=1}^n s_i (\hat{P} + \hat{R}^\top y_i - p_i) \\ &= \sum_{i=1}^n s_i \tilde{P}_o + \sum_{i=1}^n s_i (\tilde{R}_o p_i - p_i) \\ &= s_T \tilde{P}_o + s_T (\tilde{R}_o - \mathbf{I}_3) p_c \end{aligned} \quad (24)$$

Based on (8) and (24), if  $\sum_{i=1}^n s_i \tilde{y}_i \rightarrow 0$  and  $\tilde{R}_o \rightarrow \mathbf{I}_3$ , one has  $\tilde{P}_o \rightarrow 0$ . Let us summarize all the aforementioned measurements as follows:

$$\begin{cases} p_c &= \frac{1}{s_T} \sum_{i=1}^n s_i p_i, \quad s_T = \sum_{i=1}^n s_i \\ M &= \sum_{i=1}^n s_i p_i p_i^\top - s_T p_c p_c^\top \\ \tilde{R}_o M &= \sum_{i=1}^n s_i \hat{R}^\top y_i (p_i - p_c)^\top \\ \Upsilon(\tilde{R}_o M) &= \sum_{i=1}^n \frac{s_i}{2} \left( (p_i - p_c) \times \hat{R}^\top y_i \right) \\ \sum_{i=1}^n s_i \tilde{y}_i &= \sum_{i=1}^n s_i (\hat{P} + \hat{R}^\top y_i - p_i) \\ &= s_T \tilde{P}_o + s_T (\tilde{R}_o - \mathbf{I}_3) p_c \end{cases} \quad (25)$$

#### B. Direct Observer Design

The objective of the designed observer is to drive  $\hat{R} \rightarrow R$ ,  $\hat{b}_\Omega \rightarrow b_\Omega$ ,  $\hat{P} \rightarrow P$ , and  $\hat{V} \rightarrow V$  using direct measurements such that  $\lim_{t \rightarrow \infty} \tilde{R}_o = \mathbf{I}_3$  and  $\lim_{t \rightarrow \infty} \tilde{b}_\Omega = \lim_{t \rightarrow \infty} \tilde{P}_o = \lim_{t \rightarrow \infty} \tilde{V}_o = 0_{3 \times 1}$ . Consider  $\Upsilon(\tilde{R}_o M)$  and  $\sum_{i=1}^n s_i \tilde{y}_i$  are defined with respect to the direct measurements in (25):

$$\begin{aligned} \Upsilon(\tilde{R}_o M) &= \sum_{i=1}^n \frac{s_i}{2} \left( (p_i - p_c) \times \hat{R}^\top y_i \right) \\ \sum_{i=1}^n s_i \tilde{y}_i &= \sum_{i=1}^n s_i (\hat{P} + \hat{R}^\top y_i - p_i) \end{aligned}$$

Consider the following compact form of the novel direct nonlinear observer for VTOL-UAV on the Lie Group  $\hat{X} = \mathbb{SE}_2(3) \times \mathcal{U}_M \rightarrow T_{\hat{X}} \mathbb{SE}_2(3)$ :

$$\begin{cases} \dot{\hat{X}} &= \hat{X} \hat{U} - W \hat{X}, \quad \hat{U}, W \in \mathcal{U}_M, \hat{X} \in \mathbb{SE}_2(3) \\ \dot{\hat{b}}_\Omega &= \gamma_o \hat{R} \Upsilon(\tilde{R}_o M) \end{cases} \quad (26)$$

where  $\hat{X} = f(\hat{R}^\top, \hat{P}, \hat{V})$  denotes the navigation matrix estimate,  $\hat{U} = u([\Omega_m - \hat{b}_\Omega]_\times, 0_{3 \times 1}, -\frac{\mathfrak{S}}{m} e_3, 1)$ , and  $W = u([w_\Omega]_\times, w_V, w_a, 1)$ , see (5) and (6).  $J$ ,  $g$ , and  $m$  stand for vehicle's inertia matrix, gravitational acceleration, and mass, respectively. It becomes apparent that  $\hat{X}$  in (26) mimics the true VTOL-UAV motion dynamics. Also, the correction factors in  $W$  are as follows:

$$\begin{cases} w_\Omega &= k_{o1} \Upsilon(\tilde{R}_o M) \\ w_V &= k_{o2} \sum_{i=1}^n s_i \tilde{y}_i - \frac{1}{s_T} [w_\Omega]_\times \left( \sum_{i=1}^n s_i \tilde{y}_i + s_T p_c \right) \\ w_a &= -g e_3 + k_{o3} \sum_{i=1}^n s_i \tilde{y}_i \end{cases} \quad (27)$$

Furthermore,  $\gamma_o$ ,  $k_{o1}$ ,  $k_{o2}$ , and  $k_{o3}$  are positive constants. The nonlinear estimator in (26) can be detailed as follows:

$$\dot{\hat{R}} = -[\Omega_m - \hat{b}_\Omega]_\times \hat{R} + \hat{R} [w_\Omega]_\times \quad (28)$$

$$\dot{\hat{b}}_\Omega = \gamma_o \hat{R} \Upsilon(\tilde{R}_o M) \quad (29)$$

$$\dot{\hat{P}} = \hat{V} - [w_\Omega]_\times \hat{P} - w_V \quad (30)$$

$$\dot{\hat{V}} = -\frac{\mathfrak{S}}{m} \hat{R}^\top e_3 - [w_\Omega]_\times \hat{V} - w_a \quad (31)$$

**Theorem 1.** Consider the true VTOL-UAV motion dynamics in (9) and (10), and let Assumption 1 hold true where  $y_i = R(p_i - P)$  for all  $i = 1, 2, \dots, n$ . Let the observer in (26) and the correction factors in (27) be coupled with the measurements in (25). Then for  $\tilde{R}_o(0) \notin \mathcal{S}_u$ ,  $\lim_{t \rightarrow \infty} \tilde{R}_o = \mathbf{I}_3$ ,



$\lim_{t \rightarrow \infty} \tilde{b}_\Omega = \lim_{t \rightarrow \infty} \tilde{P}_o = \lim_{t \rightarrow \infty} \tilde{V}_o = 0_{3 \times 1}$ , and the closed-loop error signals are uniformly almost globally exponentially stable.

*Proof.* From (17), (9), and (28), one finds

$$\begin{aligned} \dot{\tilde{R}}_o &= \hat{R}^\top R + \hat{R}^\top \dot{R} \\ &= [\hat{R}^\top (\Omega_m - \hat{b}_\Omega) - w_\Omega] \times \tilde{R}_o - [\hat{R}^\top \Omega] \times \tilde{R}_o \\ &= -[w_\Omega - \hat{R}^\top \tilde{b}_\Omega] \times \tilde{R}_o \end{aligned} \quad (32)$$

Define  $\|\tilde{R}_o\|_I = \frac{1}{4} \text{Tr}\{\mathbf{I}_3 - \tilde{R}_o\}$  and  $\|\tilde{R}_o M\|_I = \frac{1}{4} \text{Tr}\{\mathbf{I}_3 - \tilde{R}_o\} M$ . From (3), (7), and (32), one finds [39]

$$\frac{d}{dt} \|\tilde{R}_o\|_I = -\frac{1}{2} \Upsilon(\tilde{R}_o)^\top (w_\Omega - \hat{R}^\top \tilde{b}_\Omega) \quad (33)$$

$$\frac{d}{dt} \|\tilde{R}_o M\|_I = -\frac{1}{2} \Upsilon(\tilde{R}_o M)^\top (w_\Omega - \hat{R}^\top \tilde{b}_\Omega) \quad (34)$$

Using (10), (19), and (30), one realizes that

$$\begin{aligned} \dot{\tilde{P}}_o &= \tilde{V}_o - \frac{1}{s_T} [w_\Omega] \times \sum_{i=1}^n s_i \tilde{y}_i + [w_\Omega] \times (\tilde{R}_o - \mathbf{I}_3) p_c \\ &\quad - w_V - [\hat{R}^\top \tilde{b}_\Omega] \times \tilde{R}_o P \end{aligned}$$

Using  $\dot{\tilde{P}}_o$ ,  $w_V$  in (27), and (24), one has

$$\sum_{i=1}^n s_i \dot{\tilde{y}}_i = s_T \tilde{V}_o - s_T k_{o2} \sum_{i=1}^n s_i \tilde{y}_i - s_T [\hat{R}^\top \tilde{b}_\Omega] \times \tilde{R}_o (P - p_c) \quad (35)$$

From (10), (20), (31), and using  $w_a$  in (27), one finds that

$$\begin{aligned} \dot{\tilde{V}}_o &= -[w_\Omega] \times \tilde{V}_o - k_{o3} \sum_{i=1}^n s_i \tilde{y}_i - [\hat{R}^\top \tilde{b}_\Omega] \times \tilde{R}_o V \\ &\quad + g(\mathbf{I}_3 - \tilde{R}) e_3 \end{aligned} \quad (36)$$

From (27) and (32), one is able to show that  $\Upsilon(\dot{\tilde{R}}_o) = -\frac{1}{2} \Psi(\tilde{R}_o)(w_\Omega - \hat{R}^\top \tilde{b}_\Omega)$  such that [39]

$$\Upsilon(\dot{\tilde{R}}_o) = -\frac{1}{2} \Psi(\tilde{R}_o)(k_{o1} \Upsilon(\tilde{R}_o M) - \hat{R}^\top \tilde{b}_\Omega) \quad (37)$$

where  $\Psi(\tilde{R}_o) = \text{Tr}\{\tilde{R}_o\} \mathbf{I}_3 - \tilde{R}_o$ . In view of Lemma 1, (37), and (28), one finds

$$\begin{aligned} -\frac{1}{2\delta_{o1}} \frac{d}{dt} \Upsilon(\tilde{R}_o)^\top \hat{R}^\top \tilde{b}_\Omega &\leq -\frac{1}{2\delta_{o1}} \|\hat{R}^\top \tilde{b}_\Omega\|^2 \\ &\quad + \frac{c_{o1}}{\delta_{o1}} \|\hat{R}^\top \tilde{b}_\Omega\| \sqrt{\|\tilde{R}_o\|_I} + \frac{c_{o1}}{\delta_{o1}} \|\tilde{R}_o\|_I \end{aligned} \quad (38)$$

where  $\dot{\tilde{b}}_\Omega = -\hat{b}_\Omega = -\gamma_o \hat{R} \Upsilon(\tilde{R}_o M)$ ,  $\eta_\Omega = \sup_{t \geq 0} \|\Omega\|$ , and  $c_{o1} = \max\{2(\eta_b + \sqrt{3}k_{o1} + \bar{\lambda}_M) + \eta_\Omega, 2\gamma_o \bar{\lambda}_M\}$ . Define the following Lyapunov function candidate  $\mathcal{L}_{o1} : \mathbb{S}\mathbb{O}(3) \times \mathbb{R}^3 \rightarrow \mathbb{R}_+$ :

$$\mathcal{L}_{o1} = \frac{1}{2} \text{Tr}\{(\mathbf{I}_3 - \tilde{R}_o)M\} + \frac{1}{2\gamma_o} \tilde{b}_\Omega^\top \tilde{b}_\Omega - \frac{1}{2\delta_{o1}} \Upsilon(\tilde{R}_o)^\top \hat{R}^\top \tilde{b}_\Omega \quad (39)$$

In view of (14), one has

$$e_{o1}^\top \underbrace{\begin{bmatrix} \frac{\lambda_M}{-2\delta_{o1}} & -\frac{1}{2\delta_{o1}} \\ -\frac{1}{2\delta_{o1}} & \frac{1}{2\gamma_o} \end{bmatrix}}_{Q_1} e_{o1} \leq \mathcal{L}_{o1} \leq e_{o1}^\top \underbrace{\begin{bmatrix} \frac{\bar{\lambda}_M}{2\delta_{o1}} & \frac{1}{2\delta_{o1}} \\ \frac{1}{2\delta_{o1}} & \frac{1}{2\gamma_o} \end{bmatrix}}_{Q_2} e_{o1}$$

where  $e_{o1} = [\sqrt{\|\tilde{R}_o\|_I}, \|\hat{R}^\top \tilde{b}_\Omega\|]^\top$ . It becomes evident that  $Q_1$  and  $Q_2$  can be made positive by selecting  $\delta_{o1} > \sqrt{\frac{\gamma_o}{2\lambda_M}}$ . From (29) and (34), one obtains

$$\begin{aligned} \dot{C}_o &= \frac{1}{2} \frac{d}{dt} \text{Tr}\{(\mathbf{I}_3 - \tilde{R}_o)M\} + \frac{1}{2\gamma_o} \frac{d}{dt} \tilde{b}_\Omega^\top \tilde{b}_\Omega \\ &= -\Upsilon(\tilde{R}_o M)^\top (w_\Omega - \hat{R}^\top \tilde{b}_\Omega) - \frac{1}{\gamma_o} \tilde{b}_\Omega^\top \dot{\tilde{b}}_\Omega \\ &= -k_{o1} \|\Upsilon(\tilde{R}_o M)\|^2 \\ &\leq -k_{o1} \lambda_M^2 \|\tilde{R}_o\|_I \end{aligned} \quad (40)$$

by employing (14) in Lemma 1. The result in (40) reveals that  $\dot{C}_o$  is negative and continuous,  $\dot{C}_o \rightarrow 0$  such that  $C_o \in \mathcal{L}_\infty$ , and a finite  $\lim_{t \rightarrow \infty} C_o$  exists. Hence,  $\tilde{R}_o$  and  $\tilde{b}_\Omega$  are globally bounded. Therefore,  $\dot{C}_o$  is bounded, and  $\lim_{t \rightarrow \infty} k_{o1} \|\Upsilon(\tilde{R}_o M)\| = 0_{3 \times 1}$  indicates that  $\lim_{t \rightarrow \infty} \tilde{R}_o = \mathbf{I}_3$ . The boundedness of  $\tilde{b}_\Omega$  implies that  $\tilde{R}_o$  is bounded, and on the basis of Barbalat Lemma 2,  $\lim_{t \rightarrow \infty} \dot{\tilde{R}}_o = 0_{3 \times 3}$ . Since  $\lim_{t \rightarrow \infty} \|\Upsilon(\tilde{R}_o M)\| = 0_{3 \times 1}$ , it becomes apparent that  $\lim_{t \rightarrow \infty} w_\Omega = 0_{3 \times 1}$ . Since  $\lim_{t \rightarrow \infty} \dot{\tilde{R}}_o = 0_{3 \times 3}$ ,  $\lim_{t \rightarrow \infty} -[w_\Omega - \hat{R}^\top \tilde{b}_\Omega] \times \tilde{R}_o = 0_{3 \times 3}$  showing that  $\lim_{t \rightarrow \infty} \tilde{b}_\Omega = 0_{3 \times 1}$  and, in turn,  $\lim_{t \rightarrow \infty} C_o = 0$  starting from almost any initial condition. Using (38), the derivative of (39) is:

$$\begin{aligned} \dot{\mathcal{L}}_{o1} &\leq -\left(k_{o1} \lambda_M^2 - \frac{c_{o1}}{\delta_{o1}}\right) \|\tilde{R}_o\|_I - \frac{1}{2\delta_{o1}} \|\hat{R}^\top \tilde{b}_\Omega\|^2 \\ &\quad + \frac{c_{o1}}{\delta_{o1}} \|\hat{R}^\top \tilde{b}_\Omega\| \sqrt{\|\tilde{R}_o\|_I} \end{aligned}$$

such that

$$\dot{\mathcal{L}}_{o1} \leq -\frac{1}{2\delta_{o1}} e_{o1}^\top \underbrace{\begin{bmatrix} 2k_{o1} \delta_{o1} \lambda_M^2 - 2c_{o1} & c_{o1} \\ c_{o1} & 1 \end{bmatrix}}_{D_{o1}} e_{o1} \quad (41)$$

$D_{o1}$  is made positive by setting  $\delta_{o1} > \frac{c_{o1}^2 + 2c_{o1}}{2k_{o1} \lambda_M^2}$ . Thereby, by selecting  $\delta_{o1} > \max\{\sqrt{\frac{\gamma_o}{2\lambda_M}}, \frac{c_{o1}^2 + 2c_{o1}}{2k_{o1} \lambda_M^2}\}$  and letting  $\lambda_{D_{o1}}$  be the minimum eigenvalue of  $D_{o1}$ , one finds

$$\dot{\mathcal{L}}_{o1} \leq -\lambda_{D_{o1}} (\|\tilde{R}_o\|_I + \|\hat{R}^\top \tilde{b}_\Omega\|^2) \leq -\frac{\lambda_{D_{o1}}}{\eta_o} \mathcal{L}_{o1} \quad (42)$$

where  $\eta_o = \max\{\bar{\lambda}(Q_1), \bar{\lambda}(Q_2)\}$ . From (35) and (36), define the Lyapunov function candidate  $\mathcal{L}_{o2} : \mathbb{R}^3 \times \mathbb{R}^3 \rightarrow \mathbb{R}_+$  as

$$\mathcal{L}_{o2} = \left\| \sum_{i=1}^n s_i \tilde{y}_i \right\|^2 + \frac{1}{2k_{o3}} \tilde{V}_o^\top \tilde{V}_o - \delta_{o2} \tilde{V}_o^\top \sum_{i=1}^n s_i \tilde{y}_i \quad (43)$$

One can show that

$$e_{o2}^\top \underbrace{\begin{bmatrix} \frac{1}{2} & -\frac{\delta_{o2}}{2} \\ -\frac{\delta_{o2}}{2} & \frac{1}{2k_{o3}} \end{bmatrix}}_{Q_3} e_{o2} \leq \mathcal{L}_{o2} \leq e_{o2}^\top \underbrace{\begin{bmatrix} \frac{1}{2} & \frac{\delta_{o2}}{2} \\ \frac{\delta_{o2}}{2} & \frac{1}{2k_{o3}} \end{bmatrix}}_{Q_4} e_{o2}$$

where  $e_{o2} = [\|\sum_{i=1}^n s_i \tilde{y}_i\|, \|\tilde{V}_o\|]^\top$ . One finds that  $Q_3$  and  $Q_4$  are made positive by setting  $\delta_{o2} < \frac{1}{\sqrt{k_{o3}}}$ . From (35) and (36), one finds

$$\begin{aligned} \dot{\mathcal{L}}_{o2} \leq & -e_{o2}^\top \underbrace{\begin{bmatrix} s_T k_{o2} - \delta_{o2} k_{o3} & \frac{\delta_{o2}(s_T k_{o2} + 2k_{o1} \bar{\lambda}_M)}{2} \\ \frac{\delta_{o2}(s_T k_{o2} + 2k_{o1} \bar{\lambda}_M)}{2} & s_T \delta_{o2} \end{bmatrix}}_{D_{o2}} e_{o2} \\ & + c_{o2} (\|\tilde{V}_o\| + \|\sum_{i=1}^n s_i \tilde{y}_i\|) (\|\hat{R}^\top \tilde{b}_\Omega\| + \sqrt{\|\tilde{R}_o\|_I}) \end{aligned} \quad (44)$$

where  $\eta_P = \sup_{t \geq 0} \|P - p_c\|$ ,  $\eta_V = \sup_{t \geq 0} \|V\|$ , and  $c_{o2} = \max\{s_T \eta_P \delta_{o2} + \frac{1}{k_{o3}}, \eta_V \delta_{o2} + s_T \eta_P, \frac{g}{k_{o3}}, \delta_{o2} g\}$ . It should be noted that  $\|\mathbf{I}_3 - \tilde{R}_o\|_F = 2\sqrt{2}\sqrt{\|\tilde{R}_o\|_I}$  [39]. It is evident that  $D_{o2}$  is positive if  $\delta_{o2} < \frac{4s_T^2 k_{o2}}{4s_T k_{o3} + (s_T k_{o2} + 2k_{o1} \bar{\lambda}_M)^2}$ . As such, let us select  $\delta_{o2} < \min\{\frac{1}{\sqrt{k_{o3}}}, \frac{4s_T^2 k_{o2}}{4s_T k_{o3} + (s_T k_{o2} + 2k_{o1} \bar{\lambda}_M)^2}\}$ , and let  $\lambda_{D_{o2}}$  be the minimum eigenvalue of  $D_{o2}$ . One can show that

$$\dot{\mathcal{L}}_{o2} \leq -\lambda_{D_{o2}} \|e_{o2}\|^2 + c_{o2} \|e_{o1}\| \|e_{o2}\| \quad (45)$$

From (39) and (43), define the following Lyapunov function candidate  $\mathcal{L}_{oT} : \mathbb{SO}(3) \times \mathbb{R}^3 \times \mathbb{R}^3 \times \mathbb{R}^3 \rightarrow \mathbb{R}_+$ :

$$\mathcal{L}_{oT} = \mathcal{L}_{o1} + \mathcal{L}_{o2} \quad (46)$$

From (42) and (44), one obtains

$$\begin{aligned} \dot{\mathcal{L}}_{oT} \leq & -\lambda_{D_{o1}} \|e_{o1}\|^2 - \lambda_{D_{o2}} \|e_{o2}\|^2 + c_{o2} \|e_{o1}\| \|e_{o2}\| \\ \dot{\mathcal{L}}_{oT} \leq & -\mathbf{e}_o^\top \underbrace{\begin{bmatrix} \lambda_{D_{o1}} & \frac{1}{2} c_{o2} \\ \frac{1}{2} c_{o2} & \lambda_{D_{o2}} \end{bmatrix}}_{D_o} \mathbf{e}_o \end{aligned} \quad (47)$$

with  $\mathbf{e}_o = [\|e_{o1}\|, \|e_{o2}\|]^\top$  and  $D_o$  being positive if  $\lambda_{D_{o1}} > \frac{1}{4\lambda_{D_{o2}}} c_{o2}^2$ . Let  $\lambda_{D_o}$  be the minimum eigenvalue of  $D_o$  and let  $\eta_o = \max\{\bar{\lambda}(Q_1), \bar{\lambda}(Q_2), \bar{\lambda}(Q_3), \bar{\lambda}(Q_4)\}$ . It becomes apparent that

$$\mathcal{L}_{oT}(t) \leq \mathcal{L}_{oT}(0) \exp(-\lambda_{D_o} t / \eta_o) \quad (48)$$

As such,  $\lim_{t \rightarrow \infty} \tilde{R}_o = \mathbf{I}_3$  and  $\lim_{t \rightarrow \infty} \|\tilde{b}_\Omega\| = \lim_{t \rightarrow \infty} \|\sum_{i=1}^n s_i \tilde{y}_i\| = \lim_{t \rightarrow \infty} \|\tilde{V}_o\| = 0$  exponentially. Thus,  $\|\sum_{i=1}^n s_i \tilde{y}_i\| \rightarrow 0$  implies that  $\|\tilde{P}_o\| \rightarrow 0$  exponentially, see (24). Therefore, the closed-loop error signals are almost globally exponentially stable proving Theorem 1. ■

#### IV. DIRECT OBSERVER-BASED CONTROLLER DESIGN

Let  $R_d \in \mathbb{SO}(3)$ ,  $\Omega_d \in \mathbb{R}^3$ ,  $P_d \in \mathbb{R}^3$ , and  $V_d \in \mathbb{R}^3$  denote the desired vehicle's orientation, angular velocity, position, and linear velocity, respectively. This Section aims to design an observer-based controller for a VTOL-UAV that tracks the true VTOL-UAV motion components ( $R$ ,  $\Omega$ ,  $P$ , and  $V$ ) along the desired trajectory ( $R_d$ ,  $\Omega_d$ ,  $P_d$ , and  $V_d$ ) given the information estimated ( $\tilde{R}$ ,  $\tilde{\Omega}$ ,  $\tilde{P}$ , and  $\tilde{V}$ ) by the novel direct observer as described in the previous Section along with the set of feature observation and measurement in (12) and the control inputs

$\mathcal{T} \in \mathbb{R}^3$  and  $\mathfrak{S} \in \mathbb{R}$  defined in (9) and (10). Let us define the following error components:

$$\tilde{R}_c = R_d^\top R \quad (49)$$

$$\tilde{\Omega}_c = R_d^\top (\Omega_d - \Omega) \quad (50)$$

$$\tilde{P}_c = P - P_d \quad (51)$$

$$\tilde{V}_c = V - V_d \quad (52)$$

The objective of the proposed control laws is to drive  $R \rightarrow R_d$ ,  $\Omega \rightarrow \Omega_d$ ,  $P \rightarrow P_d$ , and  $V \rightarrow V_d$  such that  $\lim_{t \rightarrow \infty} \tilde{R}_c = \mathbf{I}_3$  and  $\lim_{t \rightarrow \infty} \tilde{\Omega}_c = \lim_{t \rightarrow \infty} \tilde{P}_c = \lim_{t \rightarrow \infty} \tilde{V}_c = \mathbf{0}_{3 \times 1}$ . Recalling that  $s_T = \sum_{i=1}^n s_i$ , one finds

$$\begin{aligned} \tilde{R}_c M &= R_d^\top R M = R_d^\top \hat{R} \hat{R}^\top R M = R_d^\top \hat{R} \tilde{R}_o M \\ &= R_d^\top \sum_{i=1}^n s_i y_i (p_i - p_c)^\top \end{aligned} \quad (53)$$

where  $\tilde{R}_o M = \sum_{i=1}^n s_i \hat{R}^\top y_i (p_i - p_c)^\top$  as defined in (25). Thereby, one shows

$$\begin{aligned} \mathcal{P}_a(\tilde{R}_c M) &= \mathcal{P}_a\left(\sum_{i=1}^n s_i R_d^\top y_i (p_i - p_c)^\top\right) \\ &= \sum_{i=1}^n \frac{s_i}{2} (R_d^\top y_i (p_i - p_c)^\top - (p_i - p_c)^\top y_i^\top R_d) \end{aligned} \quad (54)$$

In view of (2),  $\Upsilon(\tilde{R}_c M) = \mathbf{vex}(\mathcal{P}_a(\tilde{R}_c M))$ . Therefore, one has

$$\Upsilon(\tilde{R}_c M) = \sum_{i=1}^n \frac{s_i}{2} ((p_i - p_c) \times R_d^\top y_i) \quad (55)$$

In view of the true rotational dynamics in (9), the desired attitude dynamics are

$$\dot{R}_d = -[\Omega_d]_\times R_d \quad (56)$$

Recall that  $\dot{V} = g e_3 - \frac{\mathfrak{S}}{m} R^\top e_3$  in (10) and re-express it  $\dot{V} = g e_3 - \frac{\mathfrak{S}}{m} R_d^\top e_3 - \frac{\mathfrak{S}}{m} (R^\top - R_d^\top) e_3 = F - \frac{\mathfrak{S}}{m} (R^\top - R_d^\top) e_3$  with  $F$  standing for an intermediary control input defined by

$$F = g e_3 - \frac{\mathfrak{S}}{m} R_d^\top e_3 = [f_1, f_2, f_3]^\top \in \mathbb{R}^3 \quad (57)$$

with  $F = [f_1, f_2, f_3]^\top \in \mathbb{R}^3$  denoting an intermediary control input to the translational dynamics described in (10) which shows that  $\mathfrak{S} = m \|g e_3 - F\|$ . Thus, the desired attitude and angular velocity will be obtained with the aid of  $F$  which allows for an explicit extraction of the desired angular velocity  $\Omega_d$  and its rate of change  $\dot{\Omega}_d$ .

**Assumption 2.** *The desired position is upper-bounded, and its first  $\dot{P}_d = V_d$ , second  $\ddot{P}_d$ , third  $P_d^{(3)}$ , and fourth  $P_d^{(4)}$  time-derivatives are upper-bounded. Also,  $\Omega_d$  and  $\dot{\Omega}_d$  are upper-bounded by a scalar  $\gamma_d < \infty$  such that  $\gamma_d \geq \max\{\sup_{t \geq 0} \|\Omega_d\|, \sup_{t \geq 0} \|\dot{\Omega}_d\|\}$ .*

**Lemma 3.** [42] *Consider the linear velocity dynamics in (10), and let  $F = [f_1, f_2, f_3]^\top \in \mathbb{R}^3$ . The thrust magnitude is  $\mathfrak{S} = m \|g e_3 - F\|$ , and the desired components of the unit-quaternion  $Q_d = [q_{d0}, q_d^\top]^\top \in \mathbb{S}^3$  are as follows:*

$$q_{d0} = \sqrt{\frac{m}{2\mathfrak{S}}(g - f_3) + \frac{1}{2}}, \quad q_d = \begin{bmatrix} \frac{m}{2\mathfrak{S}q_{d0}} f_2 \\ -\frac{m}{2\mathfrak{S}q_{d0}} f_1 \\ 0 \end{bmatrix} \quad (58)$$

given that  $F \neq [0, 0, c]^\top$  for  $c \geq g$  and  $\mathbb{S}^3 = \{Q_d \in \mathbb{R}^4 \mid \|Q_d\| = 1\}$ . Assume  $F$  is differentiable. Consequently, the desired angular velocity  $\Omega_d$  is

$$\Omega_d = \Xi(F)\dot{F} \quad (59)$$

with

$$\Xi(F) = \frac{1}{\alpha_1^2 \alpha_2} \begin{bmatrix} -f_1 f_2 & -f_2^2 + \alpha_1 \alpha_2 & f_2 \alpha_2 \\ f_1^2 - \alpha_1 \alpha_2 & f_1 f_2 & -f_1 \alpha_2 \\ f_2 \alpha_1 & -f_1 \alpha_1 & 0 \end{bmatrix} \quad (60)$$

such that  $\alpha_1 = \|ge_3 - F\|$  and  $\alpha_2 = \|ge_3 - F\| + g - f_3$ .

Lemma 3 implies that  $\mathfrak{S}$  and  $Q_d$  in (58) are singularity-free. In view of Lemma 3, the desired orientation  $R_d$  is as follows [39], [40]:

$$R_d = (q_{d0}^2 - \|q_d\|^2)\mathbf{I}_3 + 2q_d q_d^\top - 2q_{d0}[q_d]_\times \in \mathbb{SO}(3)$$

**Remark 1.**  $F$  is designed to be twice differentiable in order for the desired rate of change of angular velocity  $\dot{\Omega}_d$  to be as follows:

$$\dot{\Omega}_d = \dot{\Xi}(F)\dot{F} + \Xi(F)\ddot{F} \quad (61)$$

The derivation of  $\dot{F}$  and  $\ddot{F}$  are subsequently provided.

Consider introducing the following variables:

$$\mathcal{E} = \tilde{P}_c - \theta, \quad \dot{\mathcal{E}} = \tilde{V}_c - \dot{\theta} \quad (62)$$

with  $\theta \in \mathbb{R}^3$  describing an adaptively tuned auxiliary variable. The adaptation mechanism of  $\theta$  and the intermediary control input ( $F$ ) are designed as follows:

$$\begin{cases} \ddot{\theta} &= -k_{\theta 1} \tanh(\theta) - k_{\theta 2} \tanh(\dot{\theta}) \\ &+ k_{c3}(\hat{P} - P_d - \theta) + k_{c4}(\hat{V} - V_d - \dot{\theta}) \\ F &= \ddot{P}_d - k_{\theta 1} \tanh(\theta) - k_{\theta 2} \tanh(\dot{\theta}) \end{cases} \quad (63)$$

where  $k_{\theta 1}$ ,  $k_{\theta 2}$ ,  $k_{c3}$ , and  $k_{c4}$  denote positive constants.  $F$  is selected as in [43]. In view of (63), the first and the second derivatives of  $F$  are

$$\begin{cases} \dot{F} &= P_d^{(3)} - k_{\theta 1} H \dot{\theta} - k_{\theta 2} \dot{H} \dot{\theta} \\ \ddot{F} &= P_d^{(4)} - k_{\theta 1} Z - k_{\theta 2} \dot{Z} \end{cases} \quad (64)$$

where  $\tilde{h}(\theta_i) = 1 - \tanh^2(\theta_i)$ ,  $\tilde{h}(\dot{\theta}_i) = 1 - \tanh^2(\dot{\theta}_i)$ ,  $z_i = z(\theta_i, \dot{\theta}_i, \ddot{\theta}_i) = \tilde{h}(\theta_i)(\dot{\theta}_i - 2 \tanh(\theta_i) \dot{\theta}_i^2)$ , and  $\dot{z}_i = z(\dot{\theta}_i, \ddot{\theta}_i, \theta_i^{(3)}) = \tilde{h}(\dot{\theta}_i)(\ddot{\theta}_i - 2 \tanh(\dot{\theta}_i) \dot{\theta}_i^2)$  for all  $i = 1, 2, 3$  such that  $H = \text{diag}(\tilde{h}(\theta_1), \tilde{h}(\theta_2), \tilde{h}(\theta_3))$ ,  $\dot{H} = \text{diag}(\tilde{h}(\dot{\theta}_1), \tilde{h}(\dot{\theta}_2), \tilde{h}(\dot{\theta}_3))$ ,  $Z = [z_1, z_2, z_3]^\top$ , and  $\dot{Z} = [\dot{z}_1, \dot{z}_2, \dot{z}_3]^\top$ . Also, the third derivative  $\beta^{(3)}$  is equivalent to

$$\theta^{(3)} = -k_{\beta 1} H \dot{\theta} - k_{\theta 2} \dot{H} \dot{\theta} + k_{c1}(\hat{P} - P_d - \theta) + k_{c2}(\hat{V} - V_d - \dot{\theta})$$

In view of Lemma 3, one has  $\dot{\alpha}_1 = \frac{1}{\alpha_1} [f_1, f_2, (f_3 - g)]^\top \dot{F}$  and  $\dot{\alpha}_2 = \dot{\alpha}_1 - \dot{f}_3$  with  $\dot{F} = [\dot{f}_1, \dot{f}_2, \dot{f}_3]^\top$ . As such, it is straight forward to obtain  $\dot{\Omega}_d = \dot{\Xi}(F)\dot{F} + \Xi(F)\ddot{F}$ .

To this end, let us propose the following control laws based on the direct measurements and estimates of attitude, position, gyro bias, and linear velocity:

$$\begin{cases} \Upsilon(\tilde{R}_c M) &= \sum_{i=1}^n \frac{s_i}{2} ((p_i - p_c) \times R_d^\top y_i) \\ w_c &= k_{c1} R_d \Upsilon(\tilde{R}_c M) + k_{c2}(\Omega_d - \Omega_m + \hat{b}_\Omega) \\ \mathcal{T} &= w_c + J \dot{\Omega}_d - \left[ J(\Omega_m - \hat{b}_\Omega) \right]_\times \Omega_d \end{cases} \quad (65)$$

$$\begin{cases} \ddot{\theta} &= -k_{\theta 1} \tanh(\theta) - k_{\theta 2} \tanh(\dot{\theta}) \\ &+ k_{c3}(\hat{P} - P_d - \theta) + k_{c4}(\hat{V} - V_d - \dot{\theta}) \\ F &= \ddot{P}_d - k_{\theta 1} \tanh(\theta) - k_{\theta 2} \tanh(\dot{\theta}) \\ \mathfrak{S} &= m \|ge_3 - F\| \end{cases} \quad (66)$$

where  $\mathcal{T}$ ,  $J$ ,  $\mathfrak{S}$ ,  $F$ ,  $g$ , and  $m$  are torque input, inertia matrix, thrust magnitude, intermediary control input, gravity, and mass, respectively.  $\Omega_m$  and  $\theta \in \mathbb{R}^3$  stand for a gyro measurement and an auxiliary variable, respectively, while  $\hat{b}_\Omega$ ,  $\hat{P}$ , and  $\hat{V}$  define estimates of gyro bias, position, and linear velocity, respectively.  $k_{c1}$ ,  $k_{c2}$ ,  $k_{c3}$ ,  $k_{c4}$ ,  $k_{\theta 1}$ , and  $k_{\theta 2}$  represent positive constants. Fig. 1 presents a conceptual summary of the proposed methodology.

**Theorem 2.** Recall the dynamics in (9) and (10) and the direct observer design defined in (26). Let Assumption 2 be met and consider the control laws in (65) and (66). Then for  $\tilde{R}_o(0) \notin \mathcal{S}_u$  and  $\tilde{R}_c(0) \notin \mathcal{S}_u$ ,  $\lim_{t \rightarrow \infty} \tilde{R}_c = \tilde{R}_o = \mathbf{I}_3$ ,  $\lim_{t \rightarrow \infty} \hat{b}_\Omega = \sum_{i=1}^n s_i \tilde{y}_i = \tilde{V}_o = \mathbf{0}_{3 \times 1}$ ,  $\lim_{t \rightarrow \infty} \tilde{\Omega}_c = \lim_{t \rightarrow \infty} \tilde{P}_c = \lim_{t \rightarrow \infty} \tilde{V}_c = \mathbf{0}_{3 \times 1}$ , and the observer-based controller closed-loop error signals are uniformly almost globally exponentially stable.

*Proof.* From (49), (9) and (56), one obtains

$$\begin{aligned} \dot{\tilde{R}}_c &= \dot{R}_d^\top R + R_d^\top \dot{R} = [R_d^\top (\Omega_d - \Omega)]_\times \tilde{R}_c \\ &= [\tilde{\Omega}_c]_\times \tilde{R}_c \end{aligned} \quad (67)$$

where  $R_d^\top [\Omega]_\times R_d = [R_d^\top \Omega]_\times$ . Let us define  $\|\tilde{R}_c\|_I = \frac{1}{4} \text{Tr}\{\mathbf{I}_3 - \tilde{R}_c\}$  and  $\|\tilde{R}_c M\|_I = \frac{1}{4} \text{Tr}\{(\mathbf{I}_3 - \tilde{R}_c)M\}$ . From (3), (7), and (67), it becomes apparent that [39]

$$\frac{d}{dt} \|\tilde{R}_c\|_I = \frac{1}{2} \Upsilon(\tilde{R}_c)^\top \tilde{\Omega}_c \quad (68)$$

$$\frac{d}{dt} \|\tilde{R}_c M\|_I = \frac{1}{2} \Upsilon(\tilde{R}_c M)^\top \tilde{\Omega}_c \quad (69)$$

Using (9), (50), (67), and  $\mathcal{T}$  in (65), one finds

$$\begin{aligned} \frac{d}{dt} J R_d \tilde{\Omega}_c &= J \dot{\Omega}_d - J \dot{\Omega} \\ &= J \dot{\Omega}_d - [J \Omega]_\times R_d \tilde{\Omega}_c - [J \Omega]_\times \Omega_d - \mathcal{T} \\ &= -[J \Omega]_\times R_d \tilde{\Omega}_c - [\Omega_d]_\times J \tilde{b}_\Omega - w_c \end{aligned} \quad (70)$$

Using (51), (52), and (10), position and velocity errors are as follows:

$$\begin{cases} \dot{\tilde{P}}_c &= \tilde{V}_c \\ \dot{\tilde{V}}_c &= ge_3 - \frac{\mathfrak{S}}{m} R^\top e_3 - \dot{V}_d \end{cases} \quad (71)$$

As such, the derivatives of the variables in (62) are equivalent to

$$\begin{cases} \dot{\mathcal{E}} &= \tilde{V}_c - \dot{\theta} \\ \dot{\dot{\mathcal{E}}} &= F - \|ge_3 - F\| (R^\top - R_d^\top) e_3 - \ddot{P}_d - \ddot{\theta} \end{cases} \quad (72)$$

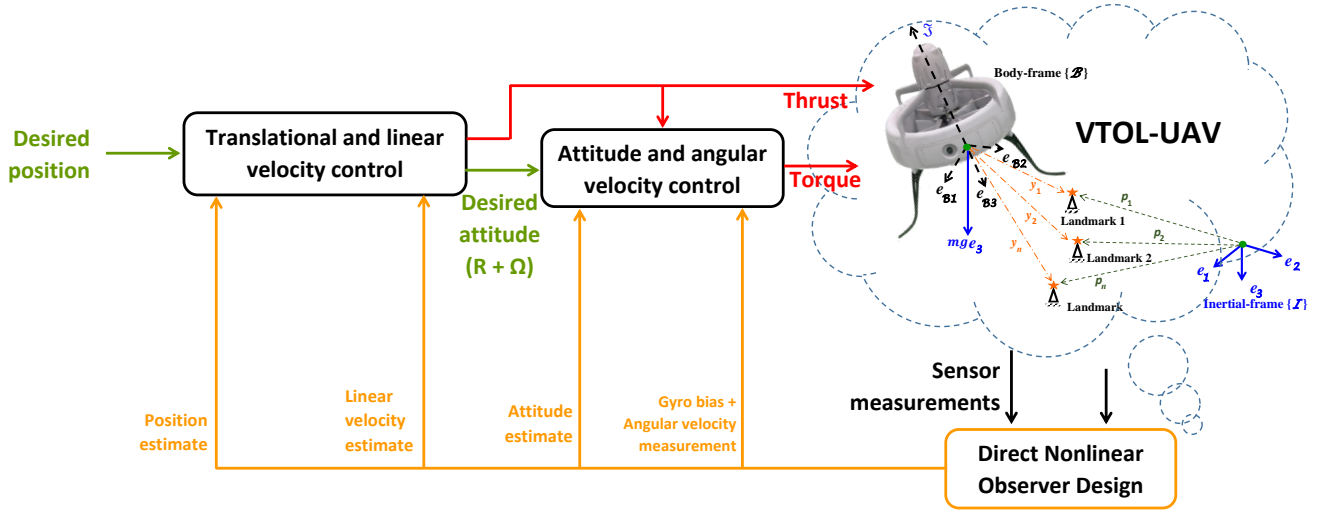


Fig. 1. Illustrative diagram of the proposed observer-based controller for VTOL-UAV.

Let us define  $C_c = \frac{1}{2} \text{Tr}\{(\mathbf{I}_3 - \tilde{R}_c)M\} + \frac{1}{2k_{c1}} \tilde{\Omega}_c^\top R_d^\top J R_d \tilde{\Omega}_c$ . (75), (76), (73), one has From (29) and (34), one obtains

$$\begin{aligned} \dot{C}_c &= \Upsilon(\tilde{R}_c M)^\top \tilde{\Omega}_c \\ &\quad - \frac{1}{k_{c1}} \tilde{\Omega}_c^\top R_d^\top ([J\Omega] \times R_d \tilde{\Omega}_c + [\Omega_d] \times J \tilde{b}_\Omega + w_c) \\ &\leq -\frac{k_{c2}}{k_{c1}} \|\tilde{\Omega}_c\|^2 + \frac{k_{c2} + \bar{\lambda}_J \eta_d}{k_{c1}} \|\tilde{\Omega}_c\| \|\tilde{b}_\Omega\| \end{aligned} \quad (73)$$

where  $\eta_d = \sup_{t \geq 0} \{\|\Omega_d\|\}$  and  $\tilde{\Omega}_c^\top R_d^\top [J\Omega] \times R_d \tilde{\Omega}_c = 0$ . In view of (48),  $\|\tilde{b}_\Omega\|$  is bounded and  $\|\tilde{b}_\Omega\| \rightarrow 0$ . As such,  $\|\tilde{\Omega}_c\|$  is bounded. The derivative of  $\Upsilon(\tilde{R}_c)$  is as follows [39]:

$$\Upsilon(\dot{\tilde{R}}_c) = \frac{1}{2} \Psi(\tilde{R}_c) \tilde{\Omega}_c \quad (74)$$

with  $\Psi(\tilde{R}_c) = \text{Tr}\{\tilde{R}_c\} \mathbf{I}_3 - \tilde{R}_c$ . Accordingly, one finds

$$\begin{aligned} &\frac{1}{\delta_{c1}} \frac{d}{dt} \Upsilon(\tilde{R}_c)^\top \tilde{\Omega}_c \\ &\leq -\frac{k_{c1} c_{c2}}{\delta_{c1}} \|\tilde{R}_c\|_I + \left( \frac{c_{c3}}{\delta_{c1}} \|\tilde{\Omega}_c\| + \frac{c_{c3}}{\delta_{c1}} \|\tilde{b}_\Omega\| \right) \sqrt{\|\tilde{R}_c\|_I} \end{aligned} \quad (75)$$

$\eta_{\Omega_c} = \sup_{t \geq 0} \{\|\tilde{\Omega}_c\|\}$ ,  $c_{c2} = \frac{\lambda_M^2}{\bar{\lambda}_J}$ , and  $c_{c3} = \max\{\frac{\eta_{\Omega_c}}{2} + c_{c1} \bar{\lambda}_M, k_{c2} + \bar{\lambda}_J \eta_d\}$ . Define the following Lyapunov function candidate  $\mathcal{L}_{c1} : \text{SO}(3) \times \mathbb{R}^3 \rightarrow \mathbb{R}_+$ :

$$\mathcal{L}_{c1} = 2\|\tilde{R}_c M\|_I + \frac{1}{2k_{c1}} \tilde{\Omega}_c^\top R_d^\top J R_d \tilde{\Omega}_c + \frac{1}{\delta_{c1}} \Upsilon(\tilde{R}_c)^\top \tilde{\Omega}_c \quad (76)$$

where

$$e_{c1}^\top \underbrace{\begin{bmatrix} \frac{\lambda_M}{2\delta_{c1}} & -\frac{1}{2k_{c1}} \\ -\frac{1}{2\delta_{c1}} & \frac{1}{2k_{c1}} \end{bmatrix}}_{Q_5} e_{c1} \leq \mathcal{L}_{c1} \leq e_{c1}^\top \underbrace{\begin{bmatrix} \frac{\lambda_M}{2\delta_{c1}} & \frac{1}{2k_{c1}} \\ \frac{1}{2\delta_{c1}} & \frac{1}{2k_{c1}} \end{bmatrix}}_{Q_6} e_{c1}$$

with  $e_{c1} = [\sqrt{\|\tilde{R}_c\|_I}, \|\tilde{\Omega}_c\|]^\top$ . It becomes obvious that  $Q_5$  and  $Q_6$  are made positive by setting  $\delta_{c1} > \sqrt{\frac{k_{c1}}{2\lambda_M}}$ . From

$$\begin{aligned} \dot{\mathcal{L}}_{c1} &\leq -e_{c1}^\top \underbrace{\begin{bmatrix} \frac{k_{c1} c_{c2}}{\delta_{c1}} & \frac{c_{c3}}{2\delta_{c1}} \\ \frac{c_{c3}}{2\delta_{c1}} & \frac{c_{c3}}{k_{c1}} \end{bmatrix}}_{D_{c1}} e_{c1} + \frac{c_{c3}}{k_{c1}} \|\tilde{\Omega}_c\| \|\tilde{b}_\Omega\| \\ &\quad + \frac{c_{c3}}{\delta_{c1}} \|\tilde{b}_\Omega\| \sqrt{\|\tilde{R}_c\|_I} \\ &\leq -\lambda_{D_{c1}} \|e_{c1}\|^2 + c_r (\|\tilde{\Omega}_c\| + \sqrt{\|\tilde{R}_c\|_I}) \|\tilde{b}_\Omega\| \end{aligned} \quad (77)$$

with  $c_r = \max\{\frac{c_{c3}}{k_{c1}}, \frac{c_{c3}}{\delta_{c1}}\}$ .  $D_{c1}$  is positive if  $\delta_{c1} > \frac{c_{c3}^2}{4c_{c2}k_{c2}}$ . Let us set  $\delta_{c1} > \max\{\sqrt{\frac{k_{c1}}{2\lambda_M}}, \frac{c_{c3}^2}{4c_{c2}k_{c2}}\}$  with  $\lambda_{D_{c1}}$  being the minimum eigenvalue of  $D_{c1}$ . Thereby, one finds

$$\mathcal{L}_{c1} \leq -\lambda_{D_{c1}} \|e_{c1}\|^2 + c_r \|e_{o1}\| \|e_{c1}\| \quad (78)$$

where  $e_{o1} = [\sqrt{\|\tilde{R}_c\|_I}, \|\hat{R}^\top \tilde{b}_\Omega\|]^\top$ . Since  $\hat{P}$ ,  $\hat{V}$ ,  $P_d$ , and  $V_d$  are bounded,  $\tilde{\theta}$  and  $F$  are bounded and, in turn,  $\Im$  is bounded. Considering the fact that  $\|\mathbf{I}_3 - \tilde{R}_c\|_F = 2\sqrt{2}\sqrt{\|\tilde{R}_c\|_I}$ , one finds that  $\|g_{e3} - F\|(R^\top - R_d^\top)e_3 \leq 4(\|g_{e3}\| + \sup_{t \geq 0} \{\|\ddot{P}_d\|\} + (k_{\theta 1} + k_{\theta 2})\sqrt{\|\tilde{R}_c\|_I}) \triangleq 4\Lambda \sqrt{\|\tilde{R}_c\|_I}$  indicating that

$$\|g_{e3} - F\|(R^\top - R_d^\top)e_3 \leq 4\Lambda \sqrt{\|\tilde{R}_c\|_I} \quad (79)$$

where  $\Lambda$  is an upper bounded positive constant. Based on (62), let us introduce the following Lyapunov function candidate  $\mathcal{L}_{c2} : \mathbb{R}^3 \times \mathbb{R}^3 \rightarrow \mathbb{R}_+$ :

$$\mathcal{L}_{c2} = \frac{1}{2} \mathcal{E}^\top \mathcal{E} + \frac{1}{2k_{c3}} \dot{\mathcal{E}}^\top \dot{\mathcal{E}} + \frac{1}{\delta_{c2}} \mathcal{E}^\top \dot{\mathcal{E}} \quad (80)$$

such that

$$e_{c2}^\top \underbrace{\begin{bmatrix} \frac{1}{2\delta_{c2}} & -\frac{1}{2k_{c3}} \\ -\frac{1}{2\delta_{c2}} & \frac{1}{2k_{c3}} \end{bmatrix}}_{Q_7} e_{c2} \leq \mathcal{L}_{c2} \leq e_{c2}^\top \underbrace{\begin{bmatrix} \frac{1}{2\delta_{c2}} & \frac{1}{2k_{c3}} \\ \frac{1}{2\delta_{c2}} & \frac{1}{2k_{c3}} \end{bmatrix}}_{Q_8} e_{c2}$$



where  $e_{c2} = [||\mathcal{E}||, ||\dot{\mathcal{E}}||]^\top$ .  $Q_7$  and  $Q_8$  can be made positive by selecting  $\delta_{c2} > \sqrt{k_{c3}}$ . Using (66), (72), and (79), one finds

$$\begin{aligned} \dot{\mathcal{L}}_{c2} \leq & -e_{c2}^\top \underbrace{\begin{bmatrix} \frac{k_{c3}}{\delta_{c2}} & \frac{k_{c4}}{2\delta_{c2}} \\ \frac{k_{c4}}{2\delta_{c2}} & \frac{k_{c4}}{k_{c3}} - \frac{1}{\delta_{c2}} \end{bmatrix}}_{D_{c2}} e_{c2} \\ & + c_m (||\mathcal{E}|| + ||\dot{\mathcal{E}}||) (||\sum_{i=1}^n s_i \tilde{y}_i|| + ||\tilde{V}_o|| + 2\sqrt{||\tilde{R}_c||_I}) \end{aligned} \quad (81)$$

with  $c_p = \max\{\sup_{t \geq 0} ||\frac{k_{c3}}{\delta_{c2}} p_c + \frac{k_{c4}}{\delta_{c2}} V||, \sup_{t \geq 0} ||p_c + \frac{k_{c4}}{k_{c3}} V||\}$  and  $c_m = \max\{\frac{1}{s_T}, \frac{k_{c4}}{k_{c3}}, \frac{k_{c3}}{\delta_{c2} s_T}, \frac{k_{c4}}{\delta_{c2}}, \frac{1}{k_{c2}}, \frac{1}{k_{c3}}, c_p, 4\Lambda\}$ . It is worth noting that  $\tilde{P}_o = \frac{1}{s_T} \sum_{i=1}^n s_i \tilde{y}_i - (\hat{R}_o - \mathbf{I}_3) p_c$ ,  $\hat{P} - P_d - \theta = -\frac{1}{s_T} \sum_{i=1}^n s_i \tilde{y}_i + (\hat{R}_o - \mathbf{I}_3) p_c + \mathcal{E}$ , and  $\hat{V} - V_d - \dot{\theta} = \tilde{V}_o + (\hat{R}_o - \mathbf{I}_3) V + \dot{\mathcal{E}}$ . Let us select  $\delta_{c2} > \frac{k_{c4}^2 + 4k_{c3}}{4k_{c4}}$  to make  $D_{c2}$  positive. Also, consider setting  $\delta_{c2} > \max\{\sqrt{k_{c3}}, \frac{k_{c4}^2 + 4k_{c3}}{4k_{c4}}\}$ . In view of (47),  $\tilde{P}_o$  and  $\tilde{V}_o$  are bounded, and based on (78),  $\sqrt{||\tilde{R}_c||_I}$  is bounded and, in turn,  $\mathcal{L}_{c2}$  is bounded. Let us use (80) and (76), and define the following Lyapunov function candidate  $\mathcal{L}_{cT} : \mathbb{SO}(3) \times \mathbb{R}^3 \times \mathbb{R}^3 \times \mathbb{R}^3 \rightarrow \mathbb{R}_+$ :

$$\mathcal{L}_{cT} = \mathcal{L}_{c1} + \mathcal{L}_{c2} \quad (82)$$

From (81) and (77), one obtains

$$\begin{aligned} \dot{\mathcal{L}}_{cT} \leq & -e_c^\top \underbrace{\begin{bmatrix} \lambda_{D_{c1}} & -c_m \\ -c_m & \lambda_{D_{c2}} \end{bmatrix}}_{D_c} e_c + c_r ||e_{o1}|| ||e_{c1}|| \\ & + c_m ||e_{o2}|| ||e_{c2}|| \end{aligned} \quad (83)$$

where  $e_c = [||e_{c1}||, ||e_{c2}||]^\top$  and  $e_{o2} = [||\sum_{i=1}^n s_i \tilde{y}_i||, ||\tilde{V}_o||]^\top$ . Select  $\lambda_{D_{c1}} > c_m^2 / \lambda_{D_{c2}}$  to make  $D_c$  positive. In view of (46) and (82), let us consider the following Lyapunov function candidate:

$$\mathcal{L}_T = \mathcal{L}_{oT} + \mathcal{L}_{cT} \quad (84)$$

Let  $c_c = \max\{c_r, c_m\}$ . Thereby, from (47) and (83), one obtains

$$\dot{\mathcal{L}}_T \leq - \begin{bmatrix} ||e_o|| \\ ||e_c|| \end{bmatrix}^\top \underbrace{\begin{bmatrix} \lambda_{D_o} & \frac{c_c}{2} \\ \frac{c_c}{2} & \lambda_{D_c} \end{bmatrix}}_D \begin{bmatrix} ||e_o|| \\ ||e_c|| \end{bmatrix} \quad (85)$$

where  $e_o = [||e_{o1}||, ||e_{o2}||]^\top$ .  $D$  can be made positive by setting  $\lambda_{D_o} > \frac{c_c^2}{4\lambda_{D_c}}$ . Hence, let us select  $\lambda_{D_o} > \frac{c_c^2}{4\lambda_{D_c}}$ . Define  $\lambda_D$  as the minimum eigenvalue of  $D$ . By letting  $\eta_Q = \max\{\bar{\lambda}(Q_1), \bar{\lambda}(Q_2), \dots, \bar{\lambda}(Q_8)\}$ , one obtains

$$\begin{aligned} \dot{\mathcal{L}}_T \leq & -\lambda_D (||\tilde{R}_o||_I + ||\tilde{b}_\Omega||^2 + ||\sum_{i=1}^n s_i \tilde{y}_i|| + ||\tilde{V}_o||^2) \\ & -\lambda_D (||\tilde{R}_c||_I + ||\tilde{\Omega}_c||^2 + |\mathcal{E}|^2 + ||\dot{\mathcal{E}}||^2) \end{aligned}$$

such that

$$\dot{\mathcal{L}}_T \leq -(\lambda_D / \eta_Q) \mathcal{L}_T(t) \quad (86)$$

and thereby

$$\mathcal{L}_T(t) \leq \mathcal{L}_T(0) \exp(-t\lambda_D / \eta_Q), \quad \forall t \geq 0 \quad (87)$$

Based on (87), it becomes apparent that  $\lim_{t \rightarrow \infty} \tilde{R}_o = \lim_{t \rightarrow \infty} \tilde{R}_c = \mathbf{I}_3$ ,  $\lim_{t \rightarrow \infty} ||\tilde{\Omega}_o|| = \lim_{t \rightarrow \infty} ||\sum_{i=1}^n s_i \tilde{y}_i|| =$

$\lim_{t \rightarrow \infty} ||\tilde{V}_o|| = 0$ , and  $\lim_{t \rightarrow \infty} ||\tilde{\Omega}_c|| = \lim_{t \rightarrow \infty} ||\mathcal{E}|| = \lim_{t \rightarrow \infty} ||\dot{\mathcal{E}}|| = 0$ . According to the definition of  $\theta$  in (66) and the convergence of  $\mathcal{L}_T(t)$  to the origin,  $\dot{\theta} \rightarrow -k_{\theta 1} \tanh(\theta) - k_{\theta 2} \tanh(\dot{\theta})$  as  $\mathcal{E}, \dot{\mathcal{E}} \rightarrow 0$  which shows that  $||\tanh(\theta)||$  and  $||\tanh(\dot{\theta})||$  are strictly decreasing with  $||\tanh(\theta)|| \rightarrow 0$  and  $||\tanh(\dot{\theta})|| \rightarrow 0$ , and therefore  $\lim_{t \rightarrow \infty} ||\theta|| = \lim_{t \rightarrow \infty} ||\dot{\theta}|| = 0$ . Thus, the closed-loop error signals of the observer-based controller design are uniformly almost globally exponentially stable. This completes the proof of Theorem 2.  $\blacksquare$

## V. IMPLEMENTATION STEPS

In this subsection, the proposed direct VTOL-UAV observer-based controller is implemented in its discrete form. Let  $\Delta t$  be a small sample time step. By following the steps below, one can seamlessly implement the novel observer-based controller.

**Step 1.** Set  $\hat{b}_{\Omega|0}, \hat{P}_0, \hat{V}_0, \theta_0, \dot{\theta}_0 \in \mathbb{R}^3, \hat{R}_0 \in \mathbb{SO}(3)$  with  $\hat{X}_0 = \begin{bmatrix} \hat{R}_0^\top & \hat{P}_0 & \hat{V}_0 \\ 0_{1 \times 3} & 1 & 0 \\ 0_{1 \times 3} & 0 & 1 \end{bmatrix}$ , and  $k = 1$ .

**Step 2.** (Thrust evaluation) Calculate the auxiliary variable  $\ddot{\theta}_k = -k_{\theta 1} \tanh(\theta_{k-1}) - k_{\theta 2} \tanh(\dot{\theta}_{k-1}) + k_{c3}(\hat{P}_k - P_{d|k} - \theta_{k-1}) + k_{c4}(\hat{V}_k - V_{d|k} - \dot{\theta}_{k-1})$  where  $\dot{\theta}_k = \dot{\theta}_{k-1} + \Delta t \ddot{\theta}_k$  and  $\theta_k = \theta_{k-1} + \Delta t \dot{\theta}_k$ . Next, evaluate the intermediary control input and the thrust as in (66)

$$\begin{aligned} F_k &= \ddot{P}_d - k_{\theta 1} \tanh(\theta_k) - k_{\theta 2} \tanh(\dot{\theta}_k) = [f_1, f_2, f_3]^\top \\ \mathfrak{S}_k &= m ||g e_3 - F_k|| \end{aligned}$$

**Step 3.** (Desired unit-quaternion) The desired unit-quaternion vector can be evaluated as in (58) by

$$q_{d0|k} = \sqrt{\frac{m}{2\mathfrak{S}_k} (g - f_3) + \frac{1}{2}}, \quad q_{d|k} = \begin{bmatrix} \frac{m}{2\mathfrak{S}_k q_{d0}} f_2 \\ -\frac{m}{2\mathfrak{S}_k q_{d0}} f_1 \\ 0 \end{bmatrix}$$

with  $F_k = [f_1, f_2, f_3]^\top \in \mathbb{R}^3, Q_{d|k} = [q_{d0|k}, q_{d|k}]^\top \in \mathbb{S}^3$ , and  $R_{d|k} = (q_{d0|k}^2 - ||q_{d|k}||^2) \mathbf{I}_3 + 2q_{d|k} q_{d|k}^\top - 2q_{d0|k} [q_{d|k}]_\times \in \mathbb{SO}(3)$

**Step 4.** (Direct sensor measurements and correction factors) Collect the following set of measurements for the observer design:

$$\begin{cases} \Upsilon(\tilde{R}_o M) &= \sum_{i=1}^n \frac{s_i}{2} ((p_i - p_c) \times \hat{R}_k^\top y_i) \\ \sum_{i=1}^n s_i \tilde{y}_i &= \sum_{i=1}^n s_i (\hat{P}_k + \hat{R}_k^\top y_i - p_i) \end{cases}$$

The correction factors can be calculated using

$$\begin{cases} w_\Omega &= k_{o1} \sum_{i=1}^n \frac{s_i}{2} ((p_i - p_c) \times \hat{R}_k^\top y_i) \\ w_V &= k_{o2} \sum_{i=1}^n s_i \tilde{y}_i - \frac{1}{s_T} [w_\Omega]_\times (\sum_{i=1}^n s_i \tilde{y}_i + s_T p_c) \\ w_a &= -g e_3 + k_{o3} \sum_{i=1}^n s_i \tilde{y}_i \end{cases}$$

**Step 5.** (Prediction) The estimates of attitude, position, and linear velocity are defined by

$$\hat{U}_k = \begin{bmatrix} [\Omega_m - \hat{b}_\Omega]_\times & 0_{3 \times 1} & -\frac{\mathfrak{S}_k}{m} e_3 \\ 0_{1 \times 3} & 0 & 0 \\ 0_{1 \times 3} & 1 & 0 \end{bmatrix} \in \mathcal{U}_{\mathcal{M}}$$

$$\hat{X}_{k|k-1} = \hat{X}_{k-1} \exp(\hat{U}_k \Delta t)$$

$\exp(\cdot)$  stands for exponential of a matrix.

$$\text{Step 6. (Correction)} \quad W = \begin{bmatrix} [w_\Omega]_\times & w_V & w_a \\ 0_{1 \times 3} & 0 & 0 \\ 0_{1 \times 3} & 1 & 0 \end{bmatrix} \in \mathcal{U}_M$$

and

$$\hat{X}_k = \exp(-W\Delta t)\hat{X}_{k|k-1}$$

with

$$\begin{aligned} \hat{P}_k &= \hat{X}_k(1:3, 4) \\ \hat{V}_k &= \hat{X}_k(1:3, 5) \\ \hat{R}_k &= \hat{X}_k(1:3, 1:3)^\top \end{aligned}$$

**Step 7.** Derivatives of the intermediary control inputs can be calculated as in (64)

$$\begin{aligned} \dot{F}_k &= P_d^{(3)} - k_{\theta 1} H \dot{\theta}_k - k_{\theta 2} \dot{H} \ddot{\theta}_k \\ \ddot{F}_k &= P_d^{(4)} - k_{\theta 1} Z - k_{\theta 2} \dot{Z} \end{aligned}$$

Next,  $\Xi(F)$  can be calculated, see (60), as well as its derivative  $\dot{\Xi}(F)$ .

**Step 8.** The desired angular velocity and its derivative can be calculated as in (59) and (61), respectively

$$\Omega_{d|k} = \Xi(F_k)\dot{F}_k, \quad \dot{\Omega}_{d|k} = \dot{\Xi}(F_k)\dot{F}_k + \Xi(F_k)\ddot{F}_k$$

**Step 9.** (Torque input) The rotational torque is defined by

$$\begin{cases} \Upsilon(\tilde{R}_c M) &= \sum_{i=1}^n \frac{s_i}{2} \left( (p_i - p_c) \times R_d^\top y_i \right) \\ w_c &= k_{c1} R_{d|k} \sum_{i=1}^n \frac{s_i}{2} \left( (p_i - p_c) \times R_{d|k}^\top y_i \right) \\ &\quad + k_{c2} (\Omega_{d|k} - \Omega_m + \hat{b}_\Omega) \\ \mathcal{T} &= w_c + J \dot{\Omega}_{d|k} - \left[ J(\Omega_m - \hat{b}_\Omega) \right]_\times \Omega_{d|k} \end{cases}$$

**Step 10.** (Gyro bias estimate) The estimate of gyro bias can be calculated using

$$\hat{b}_{\Omega|k+1} = \hat{b}_{\Omega|k} + \Delta t \gamma_o \hat{R}_k \sum_{i=1}^n \frac{s_i}{2} \left( (p_i - p_c) \times \hat{R}_k^\top y_i \right)$$

**Step 11.** Set  $k = k + 1$  and go to **Step 2**.

## VI. NUMERICAL RESULTS

In this Section, the proposed direct observer-based controller for VTOL-UAV is evaluated considering (i) a VA-INS unit at a low sampling rate of 1000 Hz, (ii) large error initialization, as well as (iii) unknown uncertain components inherent in the measurements. Let us set the initial values of the VTOL-UAV motion components as follows:

$$R_0 = \begin{bmatrix} 0.5763 & -0.7638 & 0.2907 \\ 0.8147 & 0.5085 & -0.2789 \\ 0.0652 & 0.3976 & 0.9153 \end{bmatrix} \in \mathbb{SO}(3)$$

initial position  $P_0 = [-1, -1, 0]^\top$ , initial angular velocity  $\Omega_0 = [0, 0, 0]^\top$ , and initial linear velocity  $V_0 = [1, 1, 0]^\top$ . Let the UAV mass be  $m = 3$  kg and the inertia be  $J = \text{diag}(0.15, 0.23, 0.16)$  kg·m<sup>2</sup>. Define the desired trajectory as

$$P_d = 6[\cos(0.19t), \sin(0.2t) \cos(0.2t), \frac{1}{6}(3.5 + 0.15t)]^\top \text{ m}$$

with a total travel time of 50 seconds. Let us set the initial estimates of the VTOL-UAV motion components as follows:  $\hat{R}_0 = \mathbf{I}_3$ ,  $\hat{P}_0 = \hat{V}_0 = [0, 0, 0]^\top$ , and  $\hat{b}_\Omega(0) = [0, 0, 0]^\top$ . In addition, set  $\hat{\theta}_0 = \dot{\theta}_0 = [0, 0, 0]^\top$ , and consider a set of five randomly distributed non-collinear features to satisfy Assumption 1. Let the measurements in (12) be corrupted with constant bias and normally distributed random noise with a zero mean and a standard deviation of  $0.07 = \mathcal{N}(0, 0.07)$ . Let the design parameters be selected as  $\gamma_o = 0.7$ ,  $k_{o1} = 11$ ,  $k_{o2} = 10$ ,  $k_{o3} = 4$ ,  $k_{\theta 1} = 1.2$ ,  $k_{\theta 2} = 1.2$ ,  $k_{c1} = 1$ ,  $k_{c2} = 4$ ,  $k_{c3} = 4$ , and  $k_{c4} = 2$ .

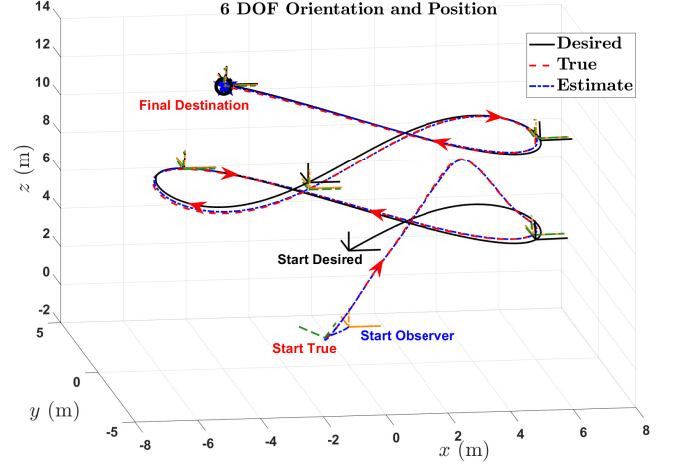


Fig. 2. Output performance of the 6 DoF VTOL-UAV observer-based controller.

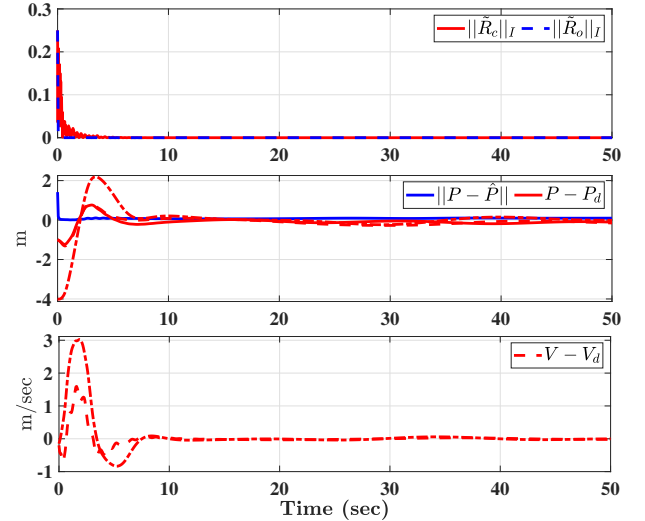


Fig. 3. Estimation and control error trajectories: attitude, angular velocity, position, linear velocity.

Fig. 2 depicts the output performance of the novel observer-based controller comparing the trajectories of the desired, true, and estimated position of the VTOL-UAV plotted in black solid line, red dashed line, and blue center line, respectively. The desired, true, and estimated VTOL-UAV orientations represented by roll, yaw, and pitch are contrasted using black

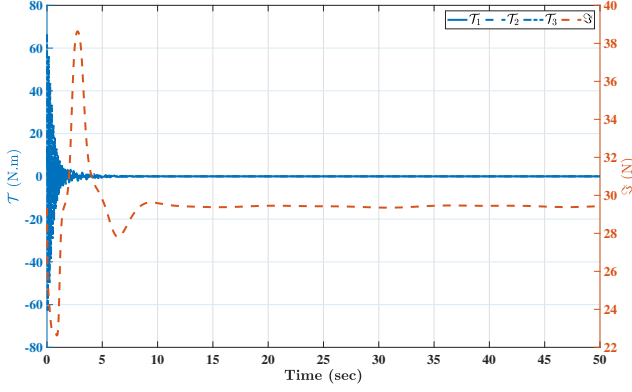


Fig. 4. VTOL-UAV control input: rotational torque and thrust.

solid line, green dashed line, and orange center-line, respectively. Fig. 2 shows robust tracking performance from a large initialization error to the desired destination. Furthermore, the convergence of the error trajectories is demonstrated in Fig. 3, where the error between the true and the estimated response plotted in blue is compared to the error between the true and the desired response plotted in red. Fig. 3 reveals fast adaptation and accurate tracking of the observer performance with respect to the true trajectory. Likewise, the fast convergence of the error signals from large values to the neighborhood of the origin in Fig. 3, illustrates the robust tracking control of the VTOL-UAV to the desired trajectory enabled by the novel observer-based controller. Fig. 4 illustrates bounded control input signals of the rotational torque and thrust.

## VII. CONCLUSION

This work tackles the estimation and control problem of a VTOL-UAV traveling in a three-dimensional space (3D) utilizing exclusively a typical 6-axis IMU (gyroscope and accelerometer) and feature measurements. This paper introduces a novel direct nonlinear observer that mimics the true nonlinearity of the VTOL-UAV motion dynamics. The proposed observer accurately estimates VTOL-UAV motion components, namely attitude, position, and linear velocity. The combination of the proposed observer with the novel control laws creates a comprehensive autonomous module, where the closed-loop error signals of both the observer and the observer-based controller are guaranteed to be exponentially stable starting from almost any initial condition. Testing of the proposed approach revealed strong tracking capabilities for the 3D motion.

## ACKNOWLEDGMENT

The authors would like to thank **Maria Shaposhnikova** for proofreading the article.

## Appendix

### Equivalent Design in Quaternion Form

Define  $Q = [q_0, q^T]^T \in \mathbb{S}^3$  to be the VTOL-UAV true unit-quaternion where  $q \in \mathbb{R}^3$  and  $q_0 \in \mathbb{R}$  with  $\mathbb{S}^3 =$

$\{Q \in \mathbb{R}^4 \mid \|Q\| = 1\}$  [39], [40]. Let  $\hat{Q} = [\hat{q}_0, \hat{q}^T]^T \in \mathbb{S}^3$  and  $Q_d = [q_{d0}, q_d^T]^T \in \mathbb{S}^3$  be the estimated and the desired unit-quaternion, respectively. Consider the mapping  $\hat{\mathcal{R}} : \mathbb{S}^3 \rightarrow \mathbb{SO}(3)$  and  $\mathcal{R}_d : \mathbb{S}^3 \rightarrow \mathbb{SO}(3)$  as [39], [40]

$$\begin{cases} \hat{\mathcal{R}} &= (\hat{q}_0^2 - \|\hat{q}\|^2)\mathbf{I}_3 + 2\hat{q}\hat{q}^T - 2\hat{q}_0[\hat{q}]_{\times} \\ \mathcal{R}_d &= (q_{d0}^2 - \|q_d\|^2)\mathbf{I}_3 + 2q_dq_d^T - 2q_{d0}[q_d]_{\times} \end{cases}$$

where  $\hat{\mathcal{R}}, \mathcal{R}_d \in \mathbb{SO}(3)$ . Recall (25) and consider the following direct measurement set-up:

$$\begin{cases} \Upsilon_o &= \mathbf{vex}(\mathcal{P}_a(\sum_{i=1}^n s_i \hat{\mathcal{R}}^T y_i (p_i - p_c)^T)) \\ \sum_{i=1}^n s_i \tilde{y}_i &= \sum_{i=1}^n s_i (\hat{P} + \hat{\mathcal{R}}^T y_i - p_i) \end{cases}$$

The unit-quaternion representation equivalent to (26) is given by

$$\begin{cases} \dot{\hat{b}}_{\Omega} &= \gamma_o \hat{\mathcal{R}} \Upsilon_o \\ w_{\Omega} &= k_{o1} \Upsilon_o \\ w_V &= k_{o2} \sum_{i=1}^n s_i \tilde{y}_i - \frac{1}{s_T} [w_{\Omega}]_{\times} (\sum_{i=1}^n s_i \tilde{y}_i + s_T p_c) \\ w_a &= -ge_3 + k_{o3} \sum_{i=1}^n s_i \tilde{y}_i \end{cases}$$

$$\begin{cases} Y &= \begin{bmatrix} 0 & -\hat{\Omega}^T \\ \hat{\Omega} & -[\hat{\Omega}]_{\times} \end{bmatrix}, \quad Z = \begin{bmatrix} 0 & -w_{\Omega}^T \\ w_{\Omega} & [w_{\Omega}]_{\times} \end{bmatrix} \\ \dot{\hat{Q}} &= \frac{1}{2}(Y - Z)\hat{Q} \\ \dot{\hat{P}} &= \hat{V} - [w_{\Omega}]_{\times} \hat{P} - w_V \\ \dot{\hat{V}} &= -\frac{\mathfrak{S}}{m} \hat{\mathcal{R}}^T e_3 - [w_{\Omega}]_{\times} \hat{V} - w_a \end{cases}$$

The control laws in (65)-(66) in terms of quaternion form are given below:

$$\begin{cases} \Upsilon_c &= \mathbf{vex}(\mathcal{P}_a(\mathcal{R}_d^T \sum_{i=1}^n s_i y_i (p_i - p_c)^T)) \\ w_c &= k_{c1} \mathcal{R}_d \Upsilon_c + k_{c2} (\Omega_d - \Omega_m + \dot{\hat{b}}_{\Omega}) \\ \mathcal{T} &= w_c + J \dot{\Omega}_d - \left[ J(\Omega_m - \dot{\hat{b}}_{\Omega}) \right]_{\times} \Omega_d \\ \ddot{\theta} &= -k_{\theta 1} \tanh(\theta) - k_{\theta 2} \tanh(\dot{\theta}) \\ &\quad + k_{c3} (\hat{P} - P_d - \theta) + k_{c4} (\hat{V} - V_d - \dot{\theta}) \\ F &= \ddot{P}_d - k_{\theta 1} \tanh(\theta) - k_{\theta 2} \tanh(\dot{\theta}) \\ \mathfrak{S} &= m \|ge_3 - F\| \end{cases}$$

## REFERENCES

- [1] H. A. Hashim, "GPS-denied navigation: Attitude, position, linear velocity, and gravity estimation with nonlinear stochastic observer," in *2021 American Control Conference (ACC)*. IEEE, 2021, pp. 1146–1151.
- [2] H. A. Hashim, M. Abouheaf, and M. A. Abido, "Geometric stochastic filter with guaranteed performance for autonomous navigation based on imu and feature sensor fusion," *Control Engineering Practice*, vol. 116, p. 104926, 2021.
- [3] D. Ivanov, M. Ovchinnikov, and D. Roldugin, "Three-axis attitude determination using magnetorquers," *Journal of Guidance, Control, and Dynamics*, vol. 41, no. 11, pp. 2455–2462, 2018.
- [4] Y. Fei, T. Meng, and Z. Jin, "Nano satellite attitude determination with randomly delayed measurements," *Acta Astronautica*, vol. 185, pp. 319–332, 2021.
- [5] J. L. Crassidis, F. L. Markley, and Y. Cheng, "Survey of nonlinear attitude estimation methods," *Journal of guidance, control, and dynamics*, vol. 30, no. 1, pp. 12–28, 2007.
- [6] X. Chen, L. Cao, P. Guo, and B. Xiao, "A higher-order robust correlation kalman filter for satellite attitude estimation," *ISA transactions*, 2019.
- [7] S. Sabzevari, M. R. Arvan, A. R. Vali, S. M. Dehghan, and M. H. Ferdowsi, "Symmetry preserving nonlinear observer for attitude estimation with magnetometer only," *ISA transactions*, vol. 102, pp. 314–324, 2020.

- [8] H. A. Hashim, "Systematic convergence of nonlinear stochastic estimators on the special orthogonal group  $SO(3)$ ," *International Journal of Robust and Nonlinear Control*, vol. 30, no. 10, pp. 3848–3870, 2020.
- [9] H. F. Grip, T. I. Fossen, T. A. Johansen, and A. Saberi, "Attitude estimation using biased gyro and vector measurements with time-varying reference vectors," *IEEE Transactions on Automatic Control*, vol. 57, no. 5, pp. 1332–1338, 2012.
- [10] H. A. Hashim, L. J. Brown, and K. McIsaac, "Nonlinear stochastic attitude filters on the special orthogonal group 3: Ito and stratonovich," *IEEE Transactions on Systems, Man, and Cybernetics: Systems*, vol. 49, no. 9, pp. 1853–1865, 2019.
- [11] D. E. Zlotnik and J. R. Forbes, "Exponential convergence of a nonlinear attitude estimator," *Automatica*, vol. 72, pp. 11–18, 2016.
- [12] H. A. Hashim and K. G. Vamvoudakis, "Adaptive neural network stochastic-filter-based controller for attitude tracking with disturbance rejection," *IEEE Transactions on Neural Networks and Learning Systems*, 2022.
- [13] H. A. Hashim, M. Abouheaf, and K. G. Vamvoudakis, "Neural-adaptive stochastic attitude filter on  $so(3)$ ," *IEEE Control Systems Letters*, vol. 6, pp. 1549–1554, 2022.
- [14] H. A. Hashim and F. L. Lewis, "Nonlinear stochastic estimators on the special euclidean group  $SE(3)$  using uncertain imu and vision measurements," *IEEE Transactions on Systems, Man, and Cybernetics: Systems*, vol. 51, no. 12, pp. 7587–7600, 2021.
- [15] N. Filipe, M. Kontitsis, and P. Tsiotras, "Extended kalman filter for spacecraft pose estimation using dual quaternions," *Journal of Guidance, Control, and Dynamics*, vol. 38, no. 9, pp. 1625–1641, 2015.
- [16] J. Wendel, O. Meister, C. Schlaile, and G. F. Trommer, "An integrated gps/mems-imu navigation system for an autonomous helicopter," *Aerospace science and technology*, vol. 10, no. 6, pp. 527–533, 2006.
- [17] G. Baldwin, R. Mahony, and J. Trumpf, "A nonlinear observer for 6 dof pose estimation from inertial and bearing measurements," in *2009 IEEE International Conference on Robotics and Automation*. IEEE, 2009, pp. 2237–2242.
- [18] H. A. Hashim, "Exponentially stable observer-based controller for VTOL-UAVs without velocity measurements," *International Journal of Control*, no. just-accepted, p. 1, 2022.
- [19] B. Xu, X. Wang, J. Zhang, and A. A. Razzaqi, "Maximum correntropy delay kalman filter for sins/usbl integrated navigation," *ISA transactions*, 2021.
- [20] R. Song, X. Chen, Y. Fang, and H. Huang, "Integrated navigation of gps/ins based on fusion of recursive maximum likelihood imm and square-root cubature kalman filter," *ISA transactions*, vol. 105, pp. 387–395, 2020.
- [21] B. Su, R. Mu, T. Long, Y. Li, and N. Cui, "Variational bayesian adaptive high-degree cubature huber-based filter for vision-aided inertial navigation on asteroid missions," *IET Radar, Sonar & Navigation*, vol. 14, no. 9, pp. 1391–1401, 2020.
- [22] A. I. Mourikis, N. Trawny, S. I. Roumeliotis, A. E. Johnson, A. Ansar, and L. Matthies, "Vision-aided inertial navigation for spacecraft entry, descent, and landing," *IEEE Transactions on Robotics*, vol. 25, no. 2, pp. 264–280, 2009.
- [23] S. Zhong and P. Chirarattananon, "Direct visual-inertial ego-motion estimation via iterated extended kalman filter," *IEEE Robotics and Automation Letters*, vol. 5, no. 2, pp. 1476–1483, 2020.
- [24] B. Allotta and et al., "An unscented kalman filter based navigation algorithm for autonomous underwater vehicles," *Mechatronics*, vol. 39, pp. 185–195, 2016.
- [25] M. Labbadi and M. Cherkaoui, "Robust adaptive backstepping fast terminal sliding mode controller for uncertain quadrotor uav," *Aerospace Science and Technology*, vol. 93, p. 105306, 2019.
- [26] F. Liao, R. Teo, J. L. Wang, X. Dong, F. Lin, and K. Peng, "Distributed formation and reconfiguration control of vtol uavs," *IEEE Transactions on Control Systems Technology*, vol. 25, no. 1, pp. 270–277, 2016.
- [27] T. Z. Muslimov and R. A. Munasypov, "Adaptive decentralized flocking control of multi-uav circular formations based on vector fields and backstepping," *ISA transactions*, vol. 107, pp. 143–159, 2020.
- [28] E.-H. Zheng, J.-J. Xiong, and J.-L. Luo, "Second order sliding mode control for a quadrotor uav," *ISA transactions*, vol. 53, no. 4, pp. 1350–1356, 2014.
- [29] X. Wu, B. Xiao, and Y. Qu, "Modeling and sliding mode-based attitude tracking control of a quadrotor uav with time-varying mass," *ISA transactions*, 2019.
- [30] X. Liang, Y. Fang, N. Sun, and H. Lin, "A novel energy-coupling-based hierarchical control approach for unmanned quadrotor transportation systems," *IEEE/ASME Transactions on Mechatronics*, vol. 24, no. 1, pp. 248–259, 2019.
- [31] I. Kaminer, A. Pascoal, E. Hallberg, and C. Silvestre, "Trajectory tracking for autonomous vehicles: An integrated approach to guidance and control," *Journal of Guidance, Control, and Dynamics*, vol. 21, no. 1, pp. 29–38, 1998.
- [32] N. Koksals, H. An, and B. Fidan, "Backstepping-based adaptive control of a quadrotor uav with guaranteed tracking performance," *ISA transactions*, vol. 105, pp. 98–110, 2020.
- [33] D. Lee, T. Ryan, and H. J. Kim, "Autonomous landing of a vtol uav on a moving platform using image-based visual servoing," in *2012 IEEE international conference on robotics and automation*. IEEE, 2012, pp. 971–976.
- [34] M. A. Rafique and A. F. Lynch, "Output-feedback image-based visual servoing for multirotor unmanned aerial vehicle line following," *IEEE Transactions on Aerospace and Electronic Systems*, vol. 56, no. 4, pp. 3182–3196, 2020.
- [35] J. Li, H. Xie, K. H. Low, J. Yong, and B. Li, "Image-based visual servoing of rotorcrafts to planar visual targets of arbitrary orientation," *IEEE Robotics and Automation Letters*, vol. 6, no. 4, pp. 7861–7868, 2021.
- [36] J. Chen, C. Hua, and X. Guan, "Image based fixed time visual servoing control for the quadrotor uav," *IET Control Theory & Applications*, vol. 13, no. 18, pp. 3117–3123, 2019.
- [37] X. Liu, J. Mao, J. Yang, S. Li, and K. Yang, "Robust predictive visual servoing control for an inertially stabilized platform with uncertain kinematics," *ISA transactions*, vol. 114, pp. 347–358, 2021.
- [38] M. R. Mokhtari, A. C. Braham, and B. Cherki, "Extended state observer based control for coaxial-rotor uav," *ISA transactions*, vol. 61, pp. 1–14, 2016.
- [39] H. A. Hashim, "Special orthogonal group  $SO(3)$ , euler angles, angle-axis, rodriguez vector and unit-quaternion: Overview, mapping and challenges," *arXiv preprint arXiv:1909.06669*, 2019.
- [40] M. D. Shuster, "A survey of attitude representations," *Navigation*, vol. 8, no. 9, pp. 439–517, 1993.
- [41] A. Barrau and S. Bonnabel, "The invariant extended kalman filter as a stable observer," *IEEE Transactions on Automatic Control*, vol. 62, no. 4, pp. 1797–1812, 2016.
- [42] A. Roberts and A. Tayebi, "Adaptive position tracking of vtol- uavs," in *Proceedings of the 48th IEEE conference on Decision and Control (CDC)*. IEEE, 2009, pp. 5233–5238.
- [43] A. Abdessameud and A. Tayebi, "Global trajectory tracking control of vtol-uavs without linear velocity measurements," *Automatica*, vol. 46, no. 6, pp. 1053–1059, 2010.